

AD-A151103

AFWAL-TR-84-3058



ENHANCED THERMAL-STRUCTURAL ANALYSIS BY  
INTEGRATED FINITE ELEMENTS

Earl A. Thornton  
and  
Pramote Dechaumphai

Department of Mechanical Engineering and Mechanics  
School of Engineering  
Old Dominion University  
Norfolk, Virginia 23508

October 1984

Final Report for the period June 1, 1982 to December 31, 1982

APPROVED FOR PUBLIC RELEASE; DISTRIBUTION UNLIMITED

FLIGHT DYNAMICS LABORATORY  
AF WRIGHT AERONAUTICAL LABORATORIES  
AIR FORCE SYSTEMS COMMAND  
WRIGHT-PATTERSON AFB, OHIO 45433

Best Available Copy

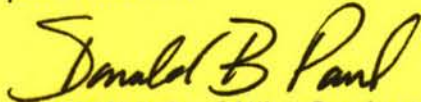
20070917049

NOTICE

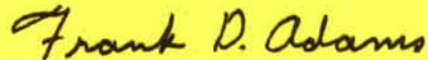
When Government drawings, specifications, or other data are used for any purpose other than in connection with a definitely related Government procurement operation, the United States Government thereby incurs no responsibility nor any obligation whatsoever; and the fact that the government may have formulated, furnished, or in any way supplied the said drawings, specifications, or other data, is not to be regarded by implication or otherwise as in any manner licensing the holder or any other person or corporation, or conveying any rights or permission to manufacture, use, or sell any patented invention that may in any way be related thereto.

This report has been reviewed by the Office of Public Affairs (ASD/PA) and is releasable to the National Technical Information Service (NTIS). At NTIS, it will be available to the general public, including foreign nations.

This technical report has been reviewed and is approved for publication.



DR DONALD B. PAUL, Project Engineer  
Structural Integrity Branch  
Structures & Dynamics Division



DR FRANK D. ADAMS, Chief  
Structural Integrity Branch  
Structures & Dynamics Division

FOR THE COMMANDER



ROGER J. HEGSTROM, Colonel, USAF  
Chief, Structures & Dynamics Division

"If your address has changed; if you wish to be removed from our mailing list, or if the addressee is no longer employed by your organization please notify AFWAL/FIBEB, W-PAFB OH 45433-6553 to help us maintain a current mailing list".

Copies of this report should not be returned unless return is required by security considerations, contractual obligations, or notice on a specific document.

REPORT DOCUMENTATION PAGE		READ INSTRUCTIONS BEFORE COMPLETING FORM
1. REPORT NUMBER AFWAL-TR-84-3058	2. GOVT ACCESSION NO.	3. RECIPIENT'S CATALOG NUMBER
4. TITLE (and Subtitle) ENHANCED THERMAL-STRUCTURAL ANALYSIS BY INTEGRATED FINITE ELEMENTS		5. TYPE OF REPORT & PERIOD COVERED Final Report - June 1, 1982- December 31, 1982
		6. PERFORMING ORG. REPORT NUMBER
7. AUTHOR(s) Earl A. Thornton, Principal Investigator and Pramote Dechaumphai, Research Associate		8. CONTRACT OR GRANT NUMBER(s) F33615-82-K-3219
9. PERFORMING ORGANIZATION NAME AND ADDRESS Old Dominion University Research Foundation P. O. Box 6369 Norfolk, Virginia 23508		10. PROGRAM ELEMENT, PROJECT, TASK AREA & WORK UNIT NUMBERS P. E. 61102F 2307-N5-24
11. CONTROLLING OFFICE NAME AND ADDRESS Flight Dynamics Laboratory (AFWAL/FIBE) AF Wright Aeronautical Laboratories, AFSC Wright-Patterson Air Force Base, Ohio 45433		12. REPORT DATE October 1984
		13. NUMBER OF PAGES 79
14. MONITORING AGENCY NAME & ADDRESS (if different from Controlling Office)		15. SECURITY CLASS. (of this report) Unclassified
		15a. DECLASSIFICATION/DOWNGRADING SCHEDULE
16. DISTRIBUTION STATEMENT (of this Report)  Approved for public release; distribution unlimited		
17. DISTRIBUTION STATEMENT (of the abstract entered in Block 20, if different from Report)		
18. SUPPLEMENTARY NOTES		
19. KEY WORDS (Continue on reverse side if necessary and identify by block number)  Thermal-structural analysis, thermal-stress analysis, finite elements, integrated analyses, hierarchical finite elements		
20. ABSTRACT (Continue on reverse side if necessary and identify by block number)  An integrated finite element approach for enhanced thermal-structural analysis is presented. The approach employs a common nodal discretization and seeks improvements in the accuracy by new hierarchical finite element formulations for the thermal and structural analyses. The effectiveness of the integrated approach is assessed for four applications with two dimensional elements. Comparative solutions show the integrated approach provides improvements in the accuracy of temperatures, displacements and thermal stresses.		

Unclassified

SECURITY CLASSIFICATION OF THIS PAGE(When Data Entered)

The applications demonstrate the practical importance of having freedom to refine each analysis independently while maintaining a common discretization. The study demonstrates that the hierarchical finite element formulations offers significant potential for the development of a general method for integrated thermal-structural analysis.

Unclassified

SECURITY CLASSIFICATION OF THIS PAGE(When Data Entered)

## FOREWORD

The project discussed in this technical report was performed under contract F33615-82-K-3219 entitled, "Basic Studies in Thermal-Structural Analysis of Large Space Structures". The contract was funded from Task 2307N5 "Basic Research in Structural Dynamics and Controls" with Dr V.B. Venkayya as the task manager. The document presents the results of research on integrated thermal structural analysis with the use of new hierarchical finite element formulations. The study was conducted at the Department of Mechanical Engineering and Mechanics, Old Dominion University, Norfolk Virginia. The work was performed under the direction of Dr Donald B. Paul, AFWAL/FIBEB, Loads & Criteria Group, Structural Integrity Branch, Structures & Dynamics Division, Flight Dynamics Laboratory of the Air Force Wright Aeronautical Laboratories Wright-Patterson AFB.

## TABLE OF CONTENTS

SECTION	PAGE
I INTRODUCTION	1
1. Background	1
2. Objectives	2
3. Scope	4
II CONVENTIONAL THERMAL-STRUCTURAL FINITE ELEMENTS	5
1. Thermal Element Formulation	5
1.1 Element Interpolation Functions	5
1.2 Element Matrices and Heat Load Vectors	6
2. Structural Element Formulation	8
2.1 Element Interpolation Functions	8
2.2 Element Stiffness Matrix and Thermal Force Vector	9
2.3 Element Stresses	12
3. Behavior of Element Thermal Stresses	12
III HIERARCHICAL THERMAL-STRUCTURAL FINITE ELEMENTS	15
1. Integrating Thermal and Structural Analyses	15
2. Improving Finite Element Approximations	17
3. The Hierarchical Approach	17
4. Comments on the Approach	21
IV NODELESS PARAMETER STRUCTURAL FINITE ELEMENTS	25
1. Rectangular Element Formulation for Linear Temperature Distribution	25
1.1 Element Interpolation Functions	25
1.2 Element Stiffness Matrix and Thermal Force Vectors	33
1.3 Element Stresses	35
2. Quadrilateral Element Formulation	35
3. Hexahedral Element Formulation	39
4. Formulation for Quadratic Temperature Distribution	44
5. Comments on Formulation	49
V APPLICATIONS	51
1. Free Expansion Plate with Linear Temperature Distribution	51

## LIST OF ILLUSTRATIONS

FIGURE		PAGE
1	Method of improving thermal-structural solution accuracy . . .	3
2	Two-dimensional conventional bilinear thermal element interpolation function . . . . .	7
3	Two-dimensional conventional structural element interpolation functions . . . . .	10
4	Deficiency of conventional finite element in predicting thermal stress distribution . . . . .	14
5	Hierarchical integrated thermal-structural analysis . . . . .	18
6	Convergence of finite element approximations . . . . .	20
7	Typical hierarchical interpolation functions for thermal analysis . . . . .	22
8	Typical hierarchical interpolation functions for structural analysis . . . . .	23
9	Rectangular structural element displacement distributions. . .	32
10	Four-node isoparametric finite element in global and natural coordinates . . . . .	36
11	Quadrilateral structural element displacement distributions. .	40
12	Eight-node isoparametric finite element in global and natural coordinates . . . . .	41
13	Comparative displacement distributions for a free expansion plate with linear temperature distribution . . . . .	53
14	Comparative thermal stress distributions for a free expansion plate with linear temperature distribution . . . . .	54
15	Conventional and nodeless parameter finite element solutions for a fixed end beam with nonlinear temperature distribution . . . . .	56
16	Hierarchical thermal-structural analysis of simplified wing section with aerodynamic heating . . . . .	58
17	Thermal-structural analysis of convectively cooled laser mirror . . . . .	62

LIST OF ILLUSTRATIONS (Cont'd)

FIGURE		PAGE
18	Typical temperature distributions at different mirror sections . . . . .	64
19	Comparative transverse displacement distributions along mirror surface . . . . .	65
20	Comparative mirror in-plane stress distributions . . . . .	66

SECTION I  
INTRODUCTION

1. Background

The determination of the structural response induced by thermal effects is an important factor in many aerospace structural designs. Extreme aerodynamic heating on advanced aerospace vehicles may produce severe thermal stresses that can reduce operational performance or even damage structures. The performance of laser devices can be degraded by thermal distortions of mirror surfaces. The thermal environment in space may cause orbiting structures to distort beyond operational tolerances. To predict the structural response accurately, effective numerical techniques capable of both thermal and structural analyses are required. One technique, the finite element method, has been found to be particularly well-suited for such analyses due to its capability to model complex geometry and to perform both thermal and structural analyses.

In predicting the thermal-structural response, basic thermal elements with assumed linear temperature distribution are frequently employed. Nodal temperatures obtained from the thermal finite element analysis are transferred to the structural finite element analysis for computations of displacements and stresses where elements with linear displacement distributions are used. This procedure, denoted as the conventional approach, is shown schematically in Figure 1(a). With the use of the elements with linear distributions in both thermal and structural analysis, a large number of elements are normally needed to produce accurate thermal-structural solutions. Often, basic differences in the thermal and structural problems mandate different analysis models, and the data transfer between the analyses

can become complicated because of the need to interpolate temperatures at the structural nodes. With increasing structural design complexity and the need for highly accurate analysis, improvements in finite element methods are needed to increase the accuracy and efficiency of coupled thermal-structural analysis.

## 2. Objectives

To improve the accuracy and efficiency of the finite element method, development of an approach called integrated thermal-structural analysis was initiated in References 1-5. The goals of the integrated approach are to: (1) provide thermal elements which predict detailed temperature distributions accurately, (2) provide structural elements with improved displacement and stress distributions which are fully compatible with the thermal elements, and (3) integrate the thermal loads with the structural analysis to further improve the accuracy of displacements and stresses. These concepts are shown schematically in Figures 1(b) and 1(c).

The goals of the integrated approach require developing new thermal and structural finite elements that can provide higher accuracy and efficiency than conventional finite elements. The task of developing new thermal elements with a common structural element discretization was begun in References 1-5. Displacements and stresses based on the new thermal elements were improved because more accurate thermal loads were provided to the structural finite element analysis.

Another task of the integrated approach is to develop new structural elements capable of providing improved displacement and stress distributions. By integrating these new structural elements with the new thermal elements developed previously, better thermal-structural solution accuracy can be obtained.

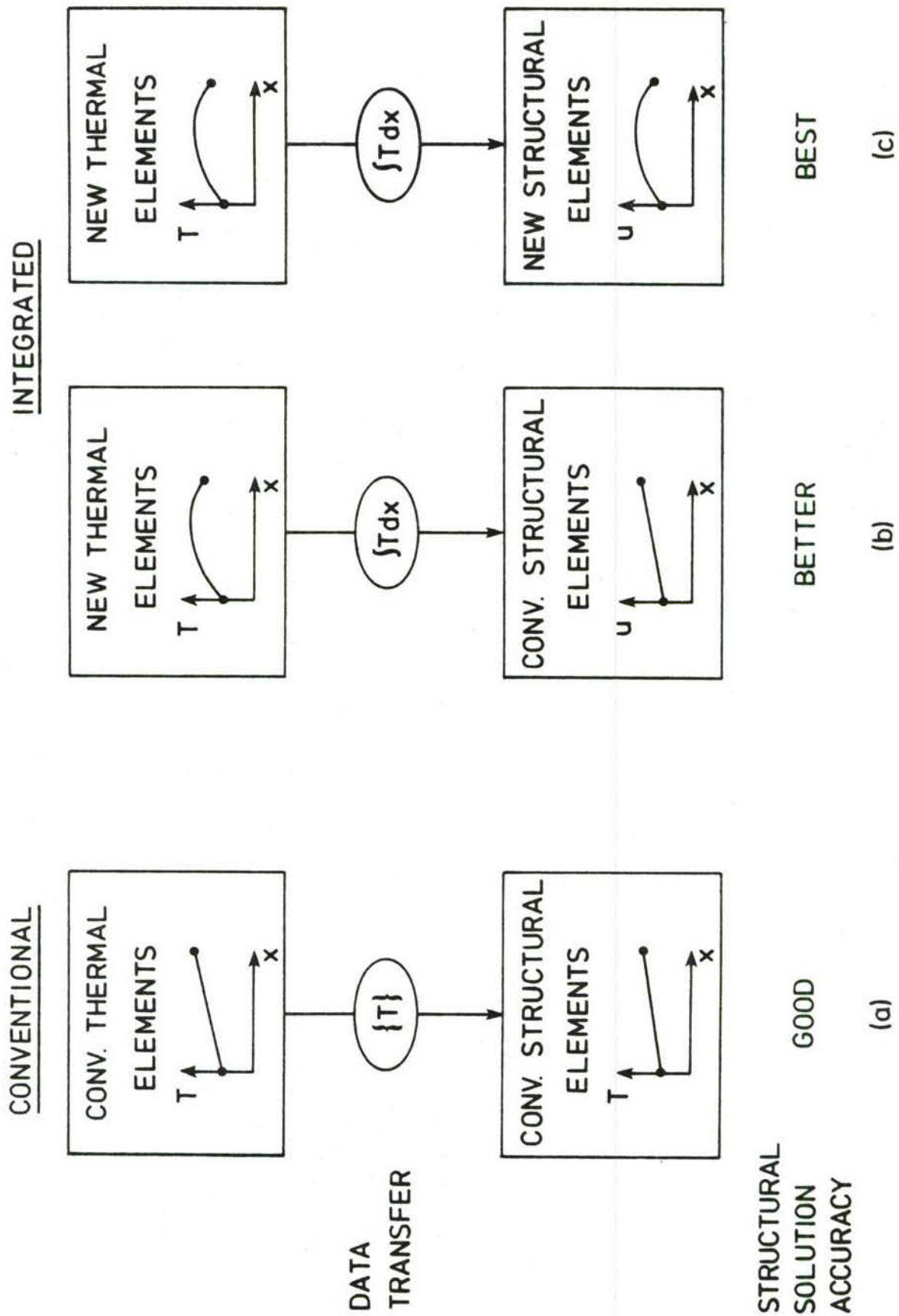


Figure 1. Method of improving thermal-structural solution accuracy.

### 3. Scope

To further develop integrated thermal-structural analysis, two procedures for developing improved thermal-structural analysis are presented. A brief review of the conventional thermal-structural finite element formulations is first given in Section II. This section describes element characteristics including some deficiencies which motivated the development of improved structural elements. The new approaches for improving the accuracy and efficiency of thermal-structural finite elements are presented in Sections III and IV. An approach using a hierarchical finite element concept is introduced in Section III, and an approach using nodeless parameter structural finite elements is introduced in Section IV. In Section V, some benefits of utilizing the new integrated thermal-structural approaches are demonstrated by numerical examples. Section VI discusses the results and highlights areas for future research.

## SECTION II

### CONVENTIONAL THERMAL-STRUCTURAL FINITE ELEMENTS

The objectives of this section are to briefly describe conventional thermal-structural finite element formulations and demonstrate the behavior of thermal stresses obtained. These basic finite element formulations will be referred to in later sections. For simplicity in understanding the thermal stress behavior, a rectangular element shape in two dimensions is used. Details of finite element formulations for general quadrilateral element shapes appear in Reference 5.

#### 1. Thermal Element Formulation

##### 1.1 Element Interpolation Functions

The element temperature distribution for a conventional bilinear four-node thermal element in local Cartesian coordinates is expressed in the form,

$$T(x,y,t) = [N_1 \quad N_2 \quad N_3 \quad N_4] \begin{Bmatrix} T_1 \\ T_2 \\ T_3 \\ T_4 \end{Bmatrix} = [N_T(x,y)]\{T(t)\} \quad (1)$$

where  $N_i$  and  $T_i$ ,  $i = 1,4$  are the element interpolation functions and the time dependent nodal temperatures, respectively. For a rectangular element, the element interpolation functions are defined by,

$$\begin{aligned} N_1 &= \left(1 - \frac{x}{a}\right)\left(1 - \frac{y}{b}\right) & N_2 &= \frac{x}{a}\left(1 - \frac{y}{b}\right) \\ N_3 &= \frac{x}{a}\frac{y}{b} & N_4 &= \left(1 - \frac{x}{a}\right)\frac{y}{b} \end{aligned} \quad (2)$$

where  $a$  and  $b$  are the element dimensions in the  $x$  and  $y$  directions. With these element interpolation functions, an element temperature distribution varies bilinearly as shown in Figure 2.

## 1.2 Element Matrices and Heat Load Vectors

Finite element (F.E.) formulations for nonlinear, transient thermal problems can be derived from the governing heat conduction equation with radiation boundary conditions by the method of weighted residuals (Reference 6). In general, the element temperature  $T(x,y,t)$  and temperature gradients are expressed in the form

$$T = [N_T]\{T(t)\}_e \quad (3a)$$

$$\begin{Bmatrix} \partial T/\partial x \\ \partial T/\partial y \end{Bmatrix} = [B_T]\{T(t)\}_e \quad (3b)$$

where  $\{T(t)\}_e$  denotes a vector of element nodal temperatures as a function of time. For simplicity, conduction with only specified surface heating and radiation heat transfer will be considered. Finite element thermal analyses for other heat loads such as internal heat generation and surface convection are presented in References 1-2. For transient thermal analysis the equations for a typical element are

$$\begin{aligned} [C]_e \dot{\{T\}}_e + [K_c]_e \{T\}_e + [K_r]_e \{T\}_e \\ = \{Q_q\}_e + \{Q_r\}_e \end{aligned} \quad (4)$$

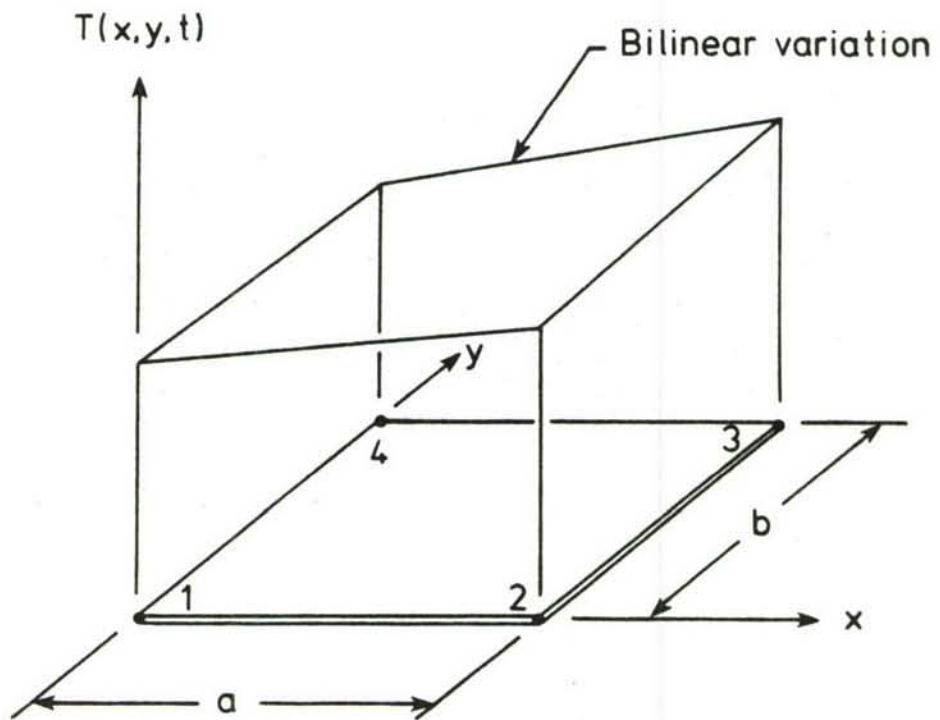


Figure 2. Two-dimensional conventional bilinear thermal element interpolation function.

where the element matrices are expressed in terms of integrals over an element volume  $V_e$  and surface  $S_e$ . The element equations are

$$[C]_e = \int_{V_e} \rho c [N_T]^T [N_T] dV \quad (5a)$$

$$[K_c]_e = \int_{V_e} [B_T]^T [k] [B_T] dV \quad (5b)$$

$$[K_r]_e \{T_e\} = \int_{S_e} \sigma \epsilon T^4 [N_T]^T dS \quad (5c)$$

$$\{Q_q\}_e = \int_{S_e} q [N_T]^T dS \quad (5d)$$

$$\{Q_r\}_e = \int_{S_e} a q_r [N_T]^T dS. \quad (5e)$$

All thermal parameters may be temperature dependent in general, but are assumed constant herein.

## 2. Structural Element Formulation

### 2.1 Element Interpolation Functions

The two-dimensional conventional bilinear four-node structural element has two in-plane displacements  $u$  and  $v$  which may vary with the element local coordinates  $x, y$  and time  $t$ . Element displacement distributions are assumed in the form,

$$\{\delta\} = \begin{Bmatrix} u(x,y,t) \\ v(x,y,t) \end{Bmatrix} = \begin{bmatrix} N_1 & 0 & N_2 & 0 & N_3 & 0 & N_4 & 0 \\ 0 & N_1 & 0 & N_2 & 0 & N_3 & 0 & N_4 \end{bmatrix} \begin{Bmatrix} u_1 \\ v_1 \\ u_2 \\ v_2 \\ u_3 \\ v_3 \\ u_4 \\ v_4 \end{Bmatrix} = [N_S]\{\delta\} \quad (6)$$

where  $N_i$ ,  $i = 1,4$  are the element displacement interpolation functions which have the same form as for the conventional finite element temperature interpolation functions shown in Equation 2. Typical element displacement distributions are shown in Figure 3.

## 2.2 Element Stiffness Matrix and Thermal Force Vector

With the assumed element displacement distributions shown in Equation 6, the element strain-displacement relations can be written as,

$$\{\epsilon\} = \begin{Bmatrix} \epsilon_x \\ \epsilon_y \\ \gamma_{xy} \end{Bmatrix} = \begin{Bmatrix} \frac{\partial u}{\partial x} \\ \frac{\partial v}{\partial y} \\ \frac{\partial u}{\partial y} + \frac{\partial v}{\partial x} \end{Bmatrix} = [B_S]\{\delta\} \quad (7)$$

where  $[B_S]$  is the strain-displacement interpolation matrix. For quasi-static analysis, the principle of minimum potential energy is applied to derive the element equations. Typical element equations may be written in the form

$$[K_S]\{\delta\} = \{F_T\} \quad (8)$$

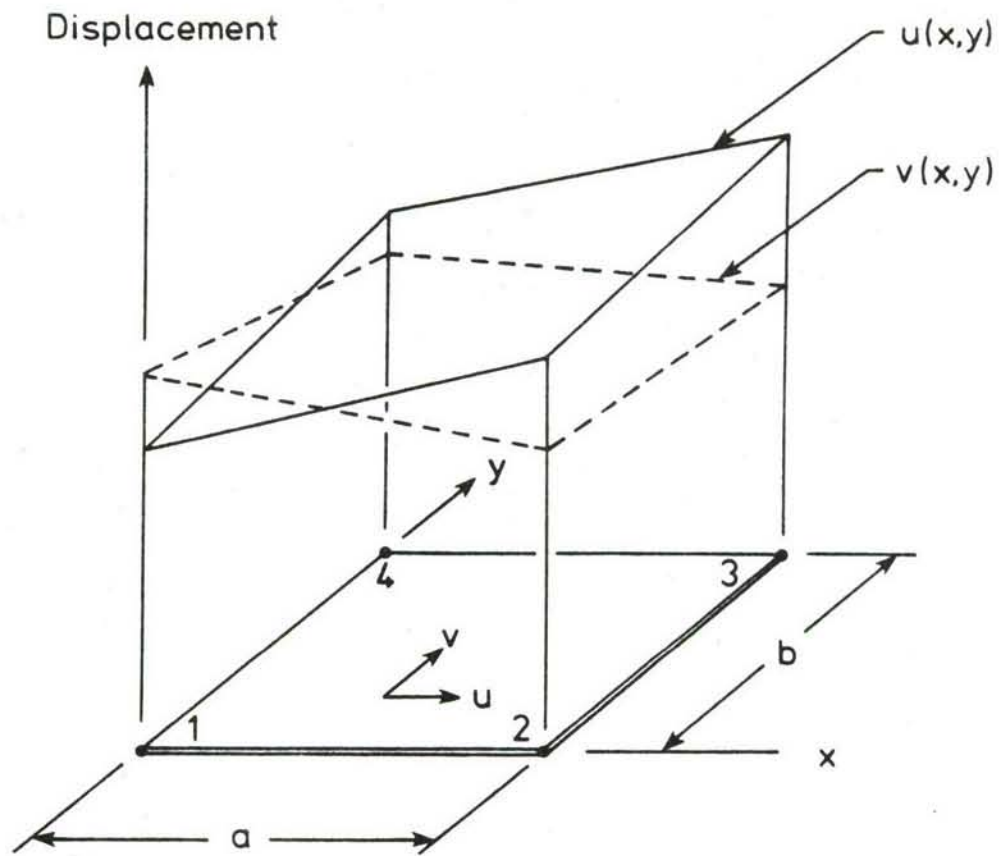


Figure 3. Two-dimensional conventional structural element interpolation functions.

where  $[K_S]$  is the element stiffness matrix, and  $\{F_T\}$  is the equivalent nodal thermal load vector. These matrices are expressed in the form of integrals over the element volume  $V$  as

$$[K_S] = \int_V [B_S]^T [D] [B_S] dV \quad (9a)$$

$$\{F_T\} = \int_V [B_S]^T [D] \{\alpha\} (T(x,y,t) - T_{ref}) dV \quad (9b)$$

where  $[D]$  is the elasticity matrix defined by (plane stress),

$$[D] = \frac{E}{1-\nu^2} \begin{bmatrix} 1 & \nu & 0 \\ \nu & 1 & 0 \\ 0 & 0 & \frac{1-\nu}{2} \end{bmatrix} \quad (10)$$

where  $\nu$  is Poisson's ratio. The vector  $\{\alpha\}$  contains the thermal expansion coefficients given by (plane stress)

$$\{\alpha\} = \begin{Bmatrix} \alpha \\ \alpha \\ 0 \end{Bmatrix} \quad (11)$$

$T(x,y,t)$  is the element temperature distribution defined in Equation 1, and  $T_{ref}$  is the reference temperature for zero stress. The elasticity matrix  $[D]$  and the vector of thermal expansion coefficients shown in the above equations can be used for plane strain by substituting  $E/(1-\nu^2)$  for  $E$ ,  $\nu(1-\nu)$  for  $\nu$ , and  $(1+\nu)\alpha$  for  $\alpha$ .

### 2.3 Element Stresses

After the element matrices shown in Equation 8 are assembled and the element nodal displacements  $\{\alpha\}$  are computed, the element stresses can be obtained using the thermo-elastic stress-strain relations,

$$\{\sigma\} = \begin{Bmatrix} \sigma_x \\ \sigma_y \\ \tau_{xy} \end{Bmatrix} = [D] \left\{ [B_s]\{\delta\} - \{\alpha\}(T(x,y,t) - T_{ref}) \right\} . \quad (12)$$

### 3. Behavior of Element Thermal Stresses

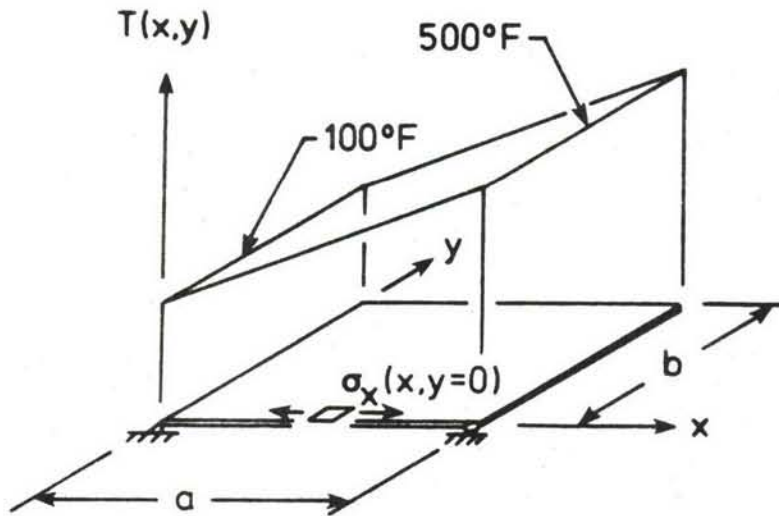
The behavior of the conventional element thermal stresses can be explained using the thermo-elastic stress-strain relations shown in Equation 12. These element stresses may be simply written in the form of the difference between element total strains and element thermal strains as

$$\begin{Bmatrix} \sigma_x \\ \sigma_y \\ \tau_{xy} \end{Bmatrix} = [D] \begin{Bmatrix} \epsilon_x - \alpha (T - T_{ref}) \\ \epsilon_y - \alpha (T - T_{ref}) \\ \gamma_{xy} - 0 \end{Bmatrix} . \quad (13)$$

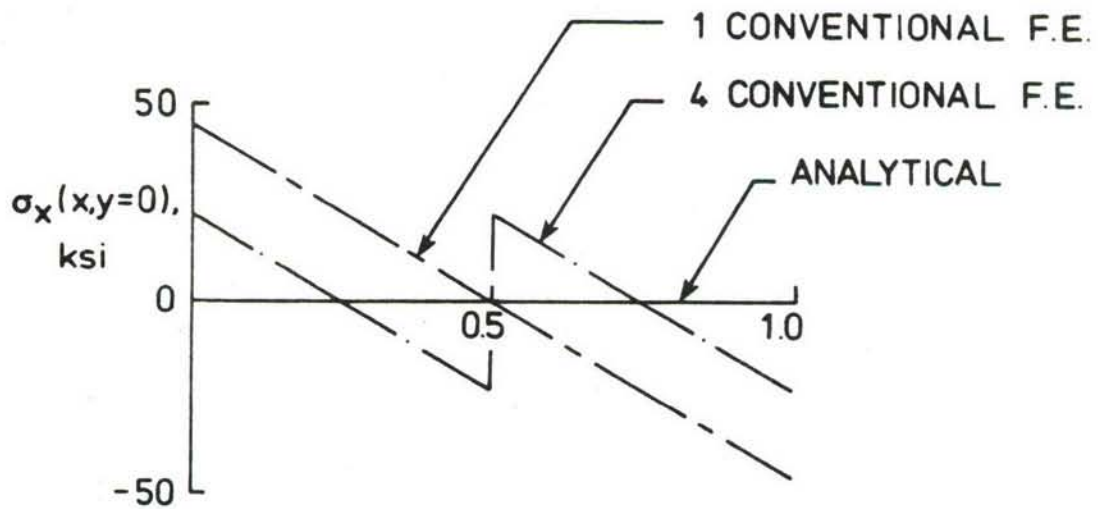
For the bilinear element displacement distributions shown in Equation 6 the total strain  $\epsilon_x$ , the derivative of the u-displacement with respect to x, is constant in the x-direction. But the thermal strain  $\alpha(T - T_{ref})$  which varies directly with the element temperature distribution is linear in the x-direction. Because the total strain and the thermal strain have different polynomial orders, unrealistic element thermal stress distributions can result.

To examine the conventional finite element thermal stress behavior, a fundamental two-dimensional thermal stress problem is analyzed. Figure 4(a) shows a plate free to expand with a prescribed linear temperature distribution. The plate is modeled by: (1) one conventional finite element, and (2) four equal conventional finite elements. Since the plate is subjected to a linear temperature distribution and is free to expand, all stress components should be zero. Figure 4(b) shows the actual distributions of the stress component  $\sigma_x$  obtained from these two finite element models. The stress distributions vary linearly within the elements and are maximum at the element boundaries, although the stresses at the element centroids are zero. By increasing the number of elements used, the element stress distributions are improved, but the stress discontinuities across the element boundaries still appear. Conventional finite elements provide accurate stresses at the element centroids in this simple example. However, the element centroidal stresses are not always conservative estimates of stresses in thermal stress problems as will be shown by examples in Section V.

It should be emphasized that the deficiency of the conventional finite element in predicting unrealistic element thermal stress distributions is because the element total strain contains a mechanical strain term one order lower than the thermal strain term. Thus, to improve the element stress distributions, the element displacement distributions should vary quadratically so that the element total strain is linear as the thermal strain.



(a) Free expansion plate with linear temperature distribution.



(b) Comparative thermal stress solution.

Figure 4. Deficiency of conventional finite element in predicting thermal stress distribution.

## SECTION III

### HIERARCHICAL THERMAL-STRUCTURAL FINITE ELEMENTS

#### 1. Integrating Thermal and Structural Analyses

To more fully develop the potential of the finite element method for thermal-stress analysis, the concept of integrated thermal-structural analysis was proposed in Reference 1. The approach focuses on aerospace applications where often thermal and structural models differ because of different analysis requirements. The objectives of the approach are to provide more efficient coupling between the thermal and structural analyses and to improve the accuracy of each analysis particularly the thermal-stress analysis. The basic philosophy of the approach is that optimum accuracy and efficiency will be achieved by working from a common geometric model and performing the analyses with the finite element method. The technology for creating geometric models within computer aided design is relatively mature and is a natural approach for initiating many interdisciplinary analyses including thermal and structural analyses. Modern computer software such as the popular PATRAN-G program are based on the concept of first developing a geometrical model and then creating the finite element discretization. The finite element method is the logical choice as the analysis method because it is inherently based on geometry.

The integrated thermal-structural approach advocated herein is based upon using the same geometric model for both analyses with a common finite element nodal discretization. The thermal and structural models are permitted to differ because heat transfer and structural response may depend on different characteristics of the system. The heat transfer problem may mandate modeling features such as insulation or cooling passages. The

structural response, however, will not depend on such non-load bearing features of the thermal model. Only in the case of conduction heat transfer with simple boundary conditions can the thermal and structural models actually be identical. Thus an integrated analysis approach must permit the use of different finite element models for the thermal and structural analyses.

A second consideration in developing integrated thermal-structural analysis is to recognize that temperature and stress distributions may be significantly different. Regions of high temperature gradients do not always correspond to regions of high stress gradients. Temperatures may vary (or not vary) significantly over a structure due to radiation boundary conditions or convective cooling. Stresses may vary significantly in a different region of the structure because of boundary constraints and geometrical effects that cause stress concentrations. Moreover, the locations of the regions of high thermal or stress gradients are not known a priori. Thus an integrated thermal-structural analysis must have the capability for independently refining the thermal and structural analysis to capture these gradients. The approach advocated for refinements is based on the use of finite element nodeless variables and hierarchical interpolation functions. Further details of this approach are given in Section III.

A third important consideration in integrated thermal-structural analysis is effectively coupling the analyses. The details of the temperature variations obtained in the thermal analysis should be employed consistently in the structural analysis to obtain the true distributions of displacement and stress. The finite element method permits consistent coupling through equivalent nodal thermal force integrals. The integrated thermal-structural

analysis approach consistently employs these integrals with the temperature representations from the thermal analysis.

## 2. Improving Finite Element Approximations

Three basic approaches for improving the quality of finite element approximations are to:

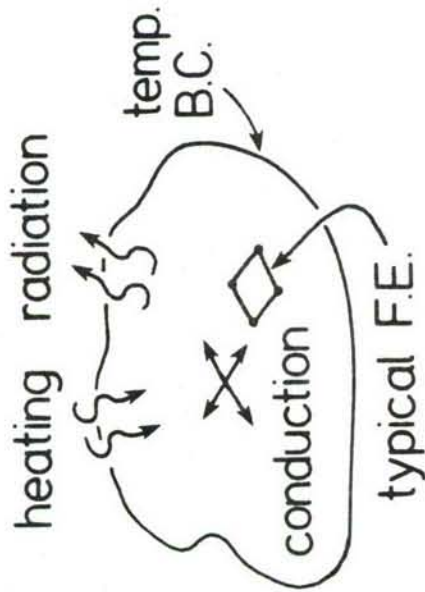
- (1) introduce additional elements of a smaller size in an area of significant dependent variable variation. This approach is called the  $h$  method where  $h$  denotes the element size, and it is the standard approach used for the solution of practical problems via standard production codes.
- (2) use the same size and definition of elements but increase the order of the interpolating polynomials. This approach is called the  $p$  method where  $p$  denotes the order of the element polynomials. With this approach additional degrees of freedom are introduced via nodeless variables. The interpolating polynomials progress in order from linear to quadratic to cubic, etc. and are called hierarchical because their contributions to the accuracy of the solution will be of diminishing importance (Reference 7).
- (3) use both  $h$  and  $p$  refinements simultaneously.

The  $h$  and  $p$  methods for improving finite element approximations are compared schematically in Figure 5.

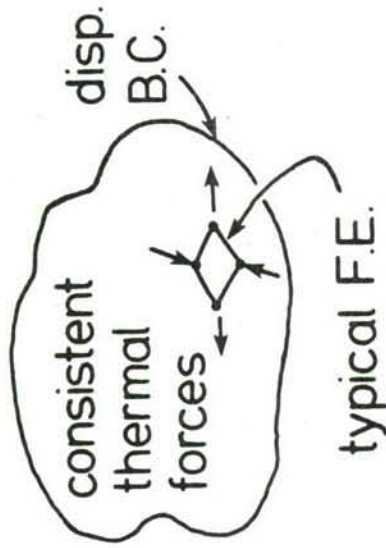
## 3. The Hierarchical Approach

The hierarchical approach of finite element analysis has been used previously to seek converged solutions for structural mechanics problems (References 8-10). Comparisons of finite element convergence via the  $h$  approach (mesh refinement) and via the  $p$  approach (increasing polynomial

## THERMAL PROBLEM



## STRUCTURAL PROBLEM



## APPROACH

1. Common discretization to suit geometry
2. Thermal solution
  - sequence of analyses (if needed)
  - accuracy improved via thermal hierarchical elements
3. Consistent thermal forces
4. Structural solution
  - sequence of analyses (if needed)
  - accuracy improved via structural hierarchical elements

Figure 5. Hierarchical integrated thermal-structure analysis.

order) are made in Reference 9, and the  $p$  approach is found to be superior. Reference 10 advocates the general adoption of the hierarchical approach and addresses questions of adaptive refinement and error estimation.

The hierarchical finite element approach for integrated thermal structural analysis uses a common discretization for the analyses and seeks improvement in the effectiveness of the analyses by: (1) improving the accuracy of the thermal analysis by using hierarchical temperature interpolation functions to converge the thermal solution, (2) using the converged temperature distribution to compute improved finite element equivalent nodal forces, (3) using hierarchical displacement functions (not necessarily the same order as the temperature interpolation functions) to converge the structural solution. The hierarchical integrated thermal-structural analysis is shown schematically in Figure 6.

In the thermal analysis, element temperatures are taken in the form

$$T(x,y,t) = \sum_{i=1}^{P_T} [N_T^i(x,y)] \{T^i(t)\} \quad (14)$$

where  $[N_T^i(x,y)]$  denote temperature interpolation functions, and  $\{T^i(t)\}$  denote vectors of unknown temperatures. For  $i = 1$ , the first term on the right hand side of Equation 14 includes the first order bilinear interpolation functions, and the vector  $\{T^1\}$  denotes the nodal temperatures. For  $i > 2$  the next terms represent the hierarchical interpolation where the superscript  $i$  denotes the order of the interpolating polynomial varying from  $i = 2$  to the highest order for the thermal analysis,  $P_T$ , and the vectors  $\{T^i\}$  for  $i > 2$  denote the nodeless variables associated with each

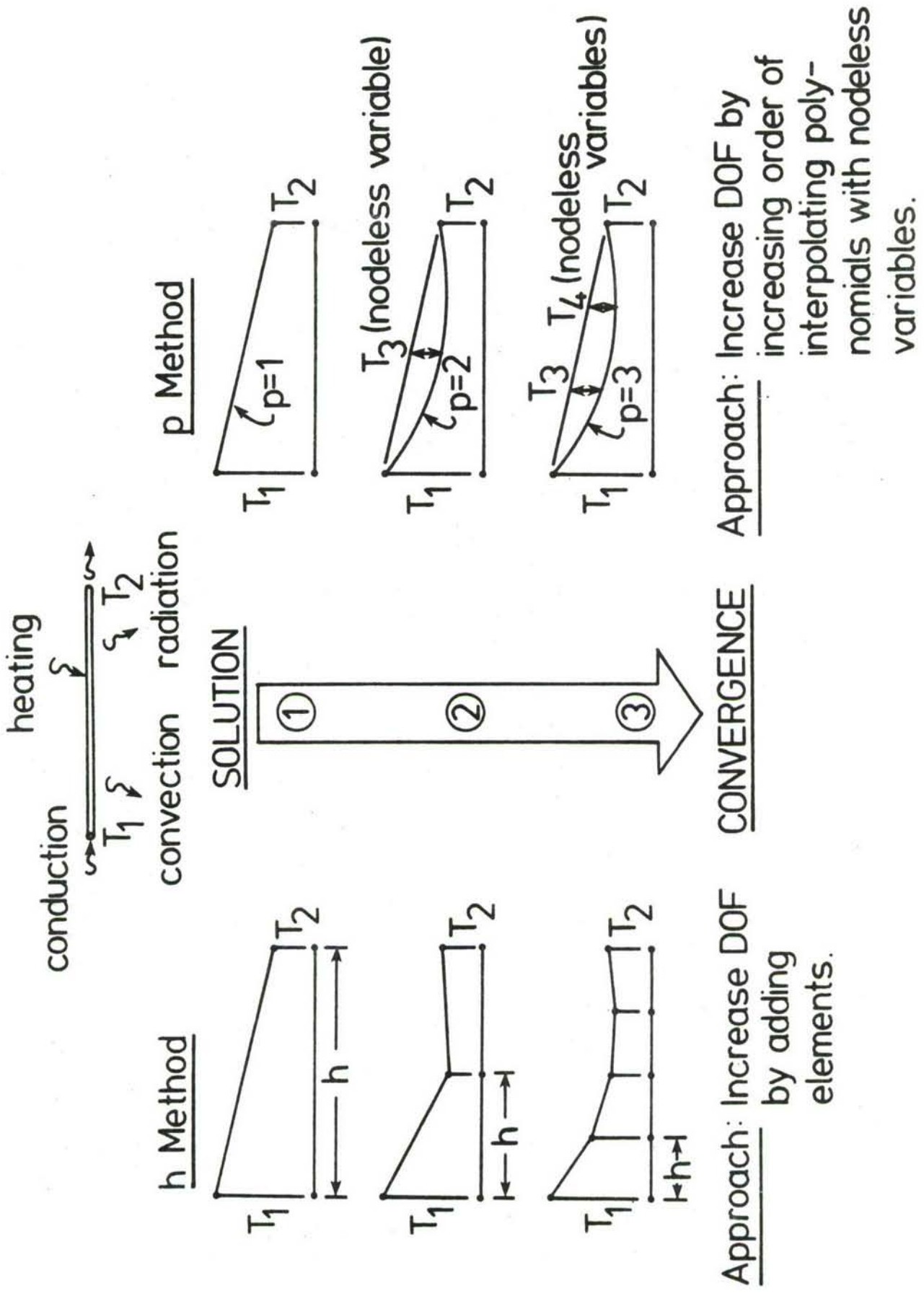


Figure 6. Convergence of finite element approximations.

interpolating polynomial. Typical hierarchical temperature interpolating polynomials and nodeless variables are shown in Figure 7.

In the structural analysis, element displacements are taken in the form

$$\{u(x,y,t)\} = \sum_{i=1}^{P_S} [N_S^i(x,y)]\{u^i(t)\} \quad (15)$$

where  $[N_S^i(x,y)]$  denote displacement interpolation functions, and  $\{u^i(t)\}$  denote vectors of unknown displacements. If  $i = 1$ , the first term on the right hand side of Equation 15 denotes the first order interpolation functions; the next terms represent the hierarchical displacement interpolation where  $i$  denotes the order of interpolating polynomial. For  $i > 2$ , the vectors  $\{u^i(t)\}$  represent the nodeless structural variables. Note that the highest order  $P_S$  for the structural analysis may differ from the highest order in the thermal analysis  $P_T$  to permit optimization of each solution independently. Typical hierarchical displacement interpolation polynomials and nodeless variables are shown in Figure 8.

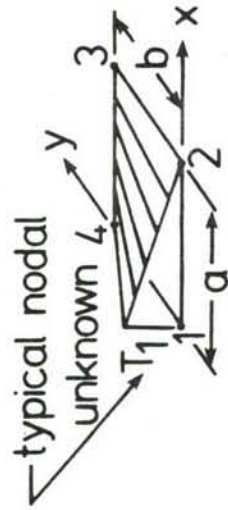
#### 4. Comments on the Approach

The hierarchical approach for integrating thermal-structural analysis is quite general and has significant potential for further development. The approach is based on using well-known finite element methodology principally from structural analysis. For example, the interpolation functions shown in Figures 7-8 are the well known Serendipity functions (Reference 6). However, a significant effort is required for the development of optimum computer programs to implement the concept. In this study only very primitive

$$T(x,y,t) = \sum_{i=1}^P N_T^i(x,y) T_i(t)$$

TYPICAL INTERPOLATION FUNCTIONS

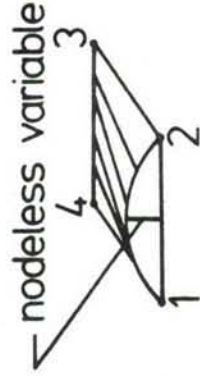
VARIABLE



BILINEAR

$$N_T^1 = \left(1 - \frac{x}{a}\right) \left(1 - \frac{y}{b}\right)$$

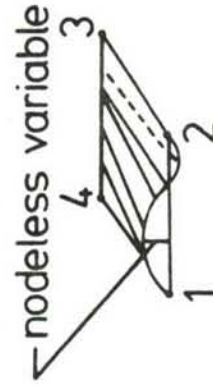
1. 1 unknown temp. per node



QUADRATIC

$$N_T^2 = \frac{4x}{a} \left(1 - \frac{x}{a}\right) \left(1 - \frac{y}{b}\right)$$

2. 1 nodeless variable per element edge



CUBIC

$$N_T^3 = \frac{9x}{a} \left(1 - \frac{x}{a}\right) \left(1 - \frac{3x}{2a}\right) \left(1 - \frac{y}{b}\right)$$

3. 2 nodeless variables per element edge

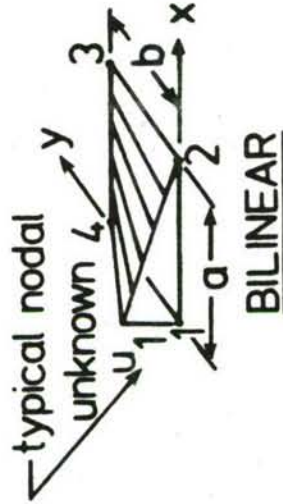
Figure 7. Typical hierarchical interpolation functions for thermal analysis.

$$P_S \{ u(x,y,t) \} = \sum_{i=1}^4 [N_S^i(x,y)] \{ u^i(t) \}$$

i      VARIABLE      TYPICAL INTERPOLATION FUNCTIONS

1. 2 unknown disp. per node

$$N_S^1 = (1 - \frac{x}{a})(1 - \frac{y}{b})$$



2. 2 nodeless variables per element edge

$$N_S^2 = \frac{4x}{a}(1 - \frac{x}{a})(1 - \frac{y}{b})$$



3. 4 nodeless variables per element edge

$$N_S^3 = \frac{9x}{a}(1 - \frac{x}{a})(1 - \frac{y}{b}) - \frac{3x^2}{2a}(1 - \frac{y}{b})$$

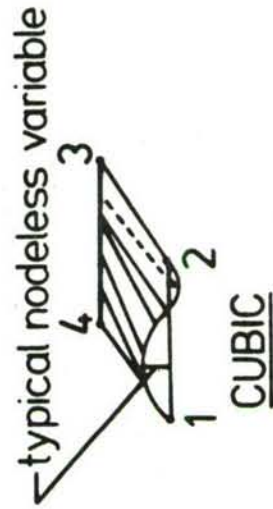


Figure 8. Typical hierarchical interpolation functions for structural analysis.

computer codes were developed for the numerical applications. No effort was made to develop efficient general codes because of the modest funding of this study. Instead exploratory programs were written to demonstrate the concept. For instance, the highest order interpolation functions implemented was quadratic.

## SECTION IV

### NODELESS PARAMETER STRUCTURAL FINITE ELEMENTS

The development of a new structural element using the nodeless parameter approach is presented in this section. The nodeless parameter approach can reduce thermal stress discontinuities between elements that are produced by conventional finite elements as demonstrated in Section II.3. The approach improves stress distributions without adding additional element unknowns. The formulation for a rectangular element with linear temperature distribution is first presented. The approach is then extended to quadrilateral and hexahedral elements. Finally, the formulation for a rectangular element with quadratic temperature distribution ( $P_T = 2$ ) is derived to demonstrate the approach for hierarchical thermal element temperature interpolation polynomials.

#### 1. Rectangular Element Formulation for Linear Temperature Distribution

##### 1.1 Element Interpolation Functions

For the one-dimensional nodeless parameter structural element presented in Reference 5, the element displacement distribution was derived from the governing differential equation of a thermo-elastic member. The displacement  $\{\bar{\delta}\}$  is written as the combination of the conventional linear displacement distribution and a displacement distribution associated with element nodal temperatures,

$$\{\bar{\delta}\} = [N_S]\{\delta\} + [\bar{N}]\{T - T_{ref}\} \quad (16)$$

where  $[N_S]$  and  $\{\delta\}$  are the conventional element displacement interpo-

lation matrix and the element nodal displacement vector, respectively. In the second term,  $[\bar{N}]$  represents the nodeless parameter interpolation matrix, and  $\{T\}$  is the vector of element nodal temperatures. The nodal temperatures are known and have the role of parameters in the structural analysis. For two- and three-dimensional problems, it is not possible to derive the element displacement distribution in a simple closed form solution from the equations of elasticity. However, the idea of assuming the element displacement distribution in the form of Equation 16 can be used where the nodeless parameter interpolation matrix  $[\bar{N}]$  is to be determined by an alternate approach.

For a two-dimensional four-node structural element, the element displacement distributions in the form of Equation 16 are,

$$\{\bar{\delta}\} = \begin{Bmatrix} u(x,y) \\ v(x,y) \end{Bmatrix} = \begin{bmatrix} N_1 & 0 & N_2 & 0 & N_3 & 0 & N_4 & 0 \\ 0 & N_1 & 0 & N_2 & 0 & N_3 & 0 & N_4 \end{bmatrix} \begin{Bmatrix} u_1 \\ v_1 \\ u_2 \\ v_2 \\ u_3 \\ v_3 \\ u_4 \\ v_4 \end{Bmatrix} + \begin{bmatrix} \bar{N}_{u1} & \bar{N}_{u2} & \bar{N}_{u3} & \bar{N}_{u4} \\ \bar{N}_{v1} & \bar{N}_{v2} & \bar{N}_{v3} & \bar{N}_{v4} \end{bmatrix} \begin{Bmatrix} T_1 - T_{ref} \\ T_2 - T_{ref} \\ T_3 - T_{ref} \\ T_4 - T_{ref} \end{Bmatrix} \quad (17)$$

where  $u$  and  $v$  are the element in-plane displacement distributions in local coordinates  $x$  and  $y$ .

For a rectangular element, the first term on the right hand side of Equation 17 represents the bilinear displacement distributions which are given by Equation 6 and are illustrated in Figure 3. With the assumed displacement distribution in the form of Equation 16, the element strain-displacement relations are

$$\{\epsilon\} = [B_S] \{\delta\} + [\bar{B}] \{T - T_{ref}\} \quad (18)$$

where  $[\bar{B}]$  is the nodeless parameter strain-displacement matrix that is to be determined. Using the thermo-elastic stress-strain relations, the element stresses are,

$$\{\sigma\} = [D] \{ [B_S] \{\delta\} + [\bar{B}] \{T - T_{ref}\} - \{\alpha\} (T(x,y) - T_{ref}) \} \quad (19)$$

In the case of the plane stress, for example, the above element stresses can be written in terms of strains as,

$$\begin{Bmatrix} \sigma_x \\ \sigma_y \\ \tau_{xy} \end{Bmatrix} = [D] \begin{Bmatrix} \epsilon_x + \bar{\epsilon}_x - \alpha (T - T_{ref}) \\ \epsilon_y + \bar{\epsilon}_y - \alpha (T - T_{ref}) \\ \gamma_{xy} + \bar{\gamma}_{xy} - 0 \end{Bmatrix} \quad (20)$$

where  $\bar{\epsilon}_x$ ,  $\bar{\epsilon}_y$  and  $\bar{\gamma}_{xy}$  are the strain components corresponding to the additional nodeless parameter interpolations introduced in Equation 16.

As mentioned in section II.3, the discontinuity of stress  $\sigma_x$  between elements is produced because the thermal strain  $\alpha T$  is one order higher algebraically than the strain  $\epsilon_x$ . The stress discontinuity can be reduced by forcing the additional strain term  $\bar{\epsilon}_x$  to have the same algebraic order as the thermal strain  $\alpha T$ , i.e.

$$\bar{\epsilon}_x(x,y) = \alpha(T(x,y) - T_{ref}) + C (T(x,y) - T_{ref}) \quad (21)$$

where  $C$  is a constant. This expression can be written explicitly as,

$$\begin{aligned} & \begin{bmatrix} \frac{\partial \bar{N}_{u1}}{\partial x} & \frac{\partial \bar{N}_{u2}}{\partial x} & \frac{\partial \bar{N}_{u3}}{\partial x} & \frac{\partial \bar{N}_{u4}}{\partial x} \end{bmatrix} \begin{pmatrix} T_1 - T_{ref} \\ T_2 - T_{ref} \\ T_3 - T_{ref} \\ T_4 - T_{ref} \end{pmatrix} \\ &= \alpha \begin{bmatrix} (1 - \frac{x}{a})(1 - \frac{y}{b}) & \frac{x}{a}(1 - \frac{y}{b}) & \frac{x}{a} \frac{y}{b} & (1 - \frac{x}{a}) \frac{y}{b} \end{bmatrix} \begin{pmatrix} T_1 - T_{ref} \\ T_2 - T_{ref} \\ T_3 - T_{ref} \\ T_4 - T_{ref} \end{pmatrix} \\ &+ [a_1 \quad b_1 \quad c_1 \quad d_1] \begin{pmatrix} T_1 - T_{ref} \\ T_2 - T_{ref} \\ T_3 - T_{ref} \\ T_4 - T_{ref} \end{pmatrix} \quad (22) \end{aligned}$$

where  $\bar{N}_{ui}$ ,  $i = 1,4$  are the nodeless parameter u-displacement interpolation functions shown in Equation 17. These interpolation functions are unknown; however, they may be determined by applying the method of undetermined coefficients to the above equation. For example, by comparing the coefficients of  $T_1$ :

$$\frac{\partial \bar{N}_{u1}}{\partial x} = \alpha \left(1 - \frac{x}{a}\right) \left(1 - \frac{y}{b}\right) + a_1$$

a solution of the nodeless parameter interpolation function  $\bar{N}_{u1}$  is,

$$\bar{N}_{u1} = \alpha \left(x - \frac{x^2}{2a}\right) \left(1 - \frac{y}{b}\right) + a_1 x + a_2$$

where  $a_1$  and  $a_2$  are constants to be determined by requiring that the displacement  $u$  be continuous between elements. To satisfy this continuity requirement, the above nodeless parameter interpolation function must vanish at  $x = 0$  and  $x = a$ , i.e.

$$\bar{N}_{u1}(x = 0, y) = 0 \tag{23}$$

$$\bar{N}_{u1}(x = a, y) = 0$$

With these two boundary conditions the constants  $a_1$  and  $a_2$  can be determined and the nodeless parameter interpolation function is obtained as,

$$\bar{N}_{u1} = \frac{\alpha}{2} \left(1 - \frac{y}{b}\right) \left(x - \frac{x^2}{a}\right) \quad (24)$$

Similarly, the unknown nodeless parameter interpolation functions  $\bar{N}_{u2}$ ,  $\bar{N}_{u3}$  and  $\bar{N}_{u4}$  can be derived using the boundary conditions given in Equation 23. Therefore, the element u-displacement distribution shown in Equation 17 becomes

$$u(x,y) = [N_1 \quad N_2 \quad N_3 \quad N_4] \begin{Bmatrix} u_1 \\ u_2 \\ u_3 \\ u_4 \end{Bmatrix} + [\bar{N}_{u1} \quad \bar{N}_{u2} \quad \bar{N}_{u3} \quad \bar{N}_{u4}] \begin{Bmatrix} T_1 - T_{ref} \\ T_2 - T_{ref} \\ T_3 - T_{ref} \\ T_4 - T_{ref} \end{Bmatrix}$$

or

$$u(x,y) = \begin{matrix} \left(1 - \frac{x}{a}\right)\left(1 - \frac{y}{b}\right) & \frac{x}{a}\left(1 - \frac{y}{b}\right) & \frac{x}{a}\frac{y}{b} & \left(1 - \frac{x}{a}\right)\frac{y}{b} \\ \frac{\alpha}{2}\left(x - \frac{x^2}{a}\right)\left(1 - \frac{y}{b}\right) & -\frac{\alpha}{2}\left(x - \frac{x^2}{a}\right)\left(1 - \frac{y}{b}\right) & -\frac{\alpha}{2}\left(x - \frac{x^2}{a}\right)\frac{y}{b} & \frac{\alpha}{2}\left(x - \frac{x^2}{a}\right)\frac{y}{b} \end{matrix} \begin{Bmatrix} u_1 \\ u_2 \\ u_3 \\ u_4 \end{Bmatrix} + \begin{matrix} \frac{\alpha}{2}\left(x - \frac{x^2}{a}\right)\left(1 - \frac{y}{b}\right) & -\frac{\alpha}{2}\left(x - \frac{x^2}{a}\right)\left(1 - \frac{y}{b}\right) & -\frac{\alpha}{2}\left(x - \frac{x^2}{a}\right)\frac{y}{b} & \frac{\alpha}{2}\left(x - \frac{x^2}{a}\right)\frac{y}{b} \end{matrix} \begin{Bmatrix} T_1 - T_{ref} \\ T_2 - T_{ref} \\ T_3 - T_{ref} \\ T_4 - T_{ref} \end{Bmatrix} \quad (25)$$

For an isothermal problem, the element u-displacement distribution shown above reduces to the bilinear distribution as assumed in the conventional element. A comparison of the u-displacement distributions for a

bilinear conventional element (Equation 6) and a nodeless parameter element (Equation 25) is shown in Figure 9(a).

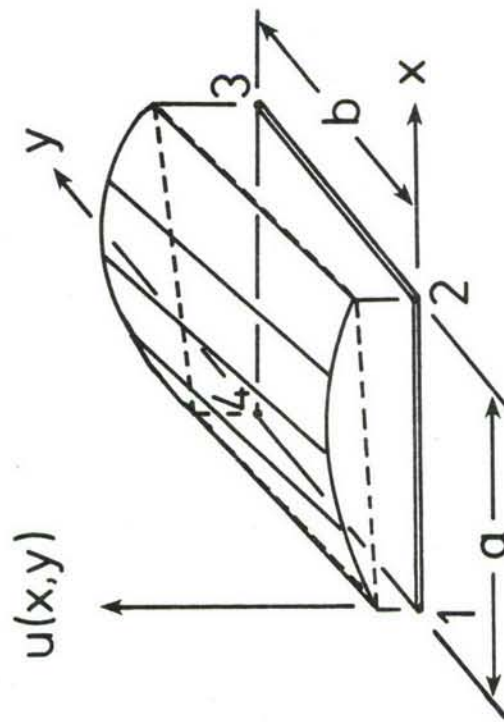
The nodeless parameter interpolation functions for the element v-displacement,  $\bar{N}_{vi}$ ,  $i = 1,4$ , can be derived using the same procedure. The appropriate boundary conditions which preserve the element v-displacement continuity are,

$$\begin{aligned}\bar{N}_{vi}(x, y=0) &= 0 \\ \bar{N}_{vi}(x, y=b) &= 0\end{aligned}\tag{26}$$

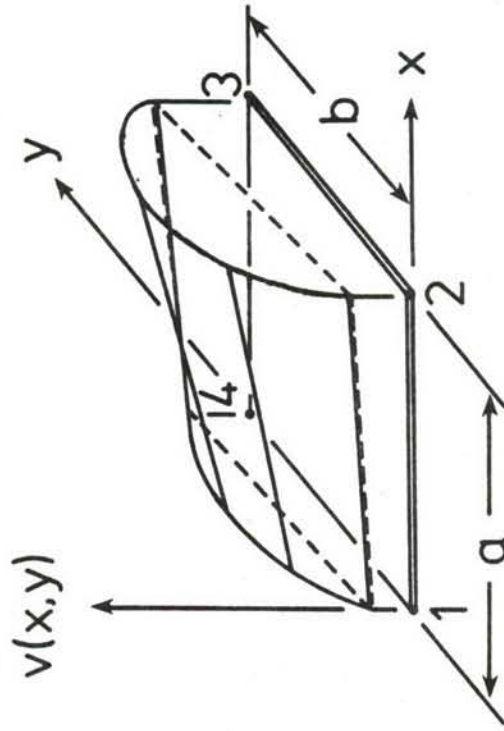
The element v-displacement distribution with nodeless parameters is

$$\begin{aligned}v(x, y) &= \begin{bmatrix} 1 - \frac{x}{a} & 1 - \frac{y}{b} & -\frac{x}{a} & 1 - \frac{y}{b} & -\frac{x}{a} & \frac{y}{b} & 1 - \frac{x}{a} & -\frac{y}{b} \end{bmatrix} \begin{Bmatrix} v_1 \\ v_2 \\ v_3 \\ v_4 \end{Bmatrix} \\ &+ \begin{bmatrix} \frac{\alpha}{2} & (1 - \frac{x}{a})(y - \frac{y^2}{b}) & -\frac{\alpha}{2} & \frac{x}{a}(y - \frac{y^2}{b}) & -\frac{\alpha}{2} & \frac{x}{a}(y - \frac{y^2}{b}) & -\frac{\alpha}{2} & \frac{x}{a}(y - \frac{y^2}{b}) \end{bmatrix} \\ &- \frac{\alpha}{2} \begin{bmatrix} (1 - \frac{x}{a})(y - \frac{y^2}{b}) \end{bmatrix} \begin{Bmatrix} T_1 - T_{ref} \\ T_2 - T_{ref} \\ T_3 - T_{ref} \\ T_4 - T_{ref} \end{Bmatrix}\end{aligned}\tag{27}$$

- Conventional bilinear displacements
- Nodeless parameter displacements for bilinear temperatures



(a)



(b)

Figure 9. Rectangular structural element displacement distributions.

The element v-displacement distribution is compared with the bilinear conventional element distribution in Figure 9(b).

## 1.2 Element Stiffness Matrix and Thermal Force Vectors

Finite element equations and element matrices can be derived by applying the principle of minimum potential energy (Reference 6). For simplicity in the derivation here, the effects of external applied forces are not included; only thermal effects are considered.

The total potential energy is represented by the internal strain energy written in the form,

$$\Pi = \frac{1}{2} \int_V [\epsilon - \epsilon_0] \{\sigma\} dV \quad (28)$$

where  $V$  is the element volume, and  $\{\sigma\}$  denotes the vector of stress components;  $[\epsilon]$  denotes the row matrix of the total strain components shown in Equation 18, and  $[\epsilon_0]$  denotes the row matrix of the thermal strain components. For example, the vector of thermal strain components for the plane stress problem is,

$$\{\epsilon_0\} = \{\alpha\} (T - T_{ref}) = \begin{Bmatrix} \alpha (T - T_{ref}) \\ \alpha (T - T_{ref}) \\ 0 \end{Bmatrix} \quad (29)$$

Using the stress-strain relations,

$$\{\sigma\} = [D] \{\epsilon - \epsilon_0\} \quad (30)$$

the total potential energy, Equation 28, becomes

$$\Pi = \frac{1}{2} \int_V [\epsilon - \epsilon_0] [D] \{\epsilon - \epsilon_0\} dV \quad (31)$$

By substituting the strain-displacement relations for the nodeless parameter element, Equation 18, the total potential energy can be written in the form,

$$\begin{aligned} \Pi = & \frac{1}{2} \{\delta\}^T \int_V [B_S]^T [D] [B_S] dV \{\delta\} - \{\delta\}^T \int_V [B_S]^T [D] \{\epsilon_0\} dV \\ & + \frac{1}{2} \int_V [\epsilon_0] [D] \{\epsilon_0\} dV + \{\delta\}^T \int_V [B_S]^T [D] [\bar{B}] \{T - T_{ref}\} dV \end{aligned} \quad (32)$$

The element equilibrium equations are then derived by performing the minimization of the total potential energy with respect to element modal unknowns. The equilibrium equations have the form,

$$[K_S] \{\delta\} = \{F_T\} - \{\bar{F}_T\} \quad (33)$$

where  $[K_S]$  and  $\{F_T\}$  are the element stiffness matrix and the equivalent nodal thermal load vector, respectively. These two element matrices are identical to those obtained from the conventional element formulation given in Equation 9a and 9b, respectively. The vector  $\{\bar{F}_T\}$  is produced by the element nodeless parameter interpolation functions and is given by

$$\{\bar{F}_T\} = \int_V [B_S]^T [D] [\bar{B}] \{T - T_{ref}\} dV \quad (34)$$

As shown by the element equilibrium equations, the nodeless parameter approach does not require extra element unknowns or modify the stiffness matrix, however, an additional element nodal force vector  $\{\bar{F}_T\}$  is introduced. Due to this additional element nodal force vector, nodal displacements computed are different in general from the conventional finite element solution.

### 1.3 Element Stresses

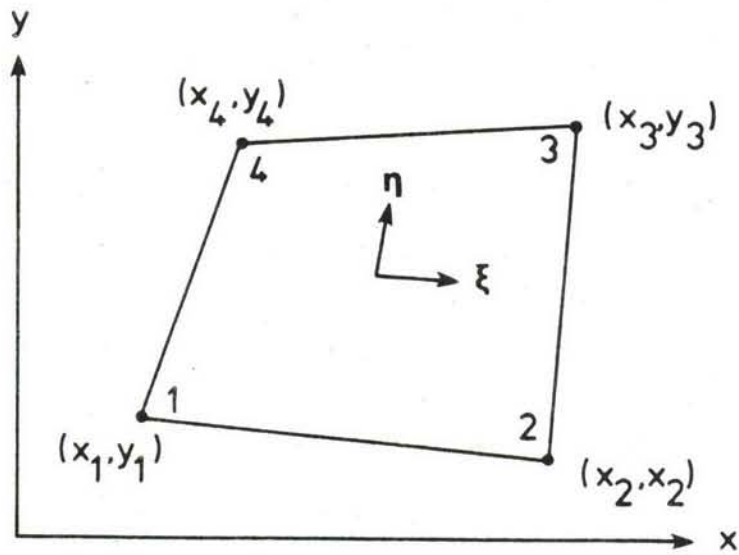
Once element nodal displacements  $\{\delta\}$  are obtained, element stresses can be computed from the thermo-elastic stress-strain relations,

$$\{\sigma\} = [D] \{ [B_S] \{\delta\} + [B] \{T - T_{ref}\} - \{\alpha\} (T - T_{ref}) \} \quad (35)$$

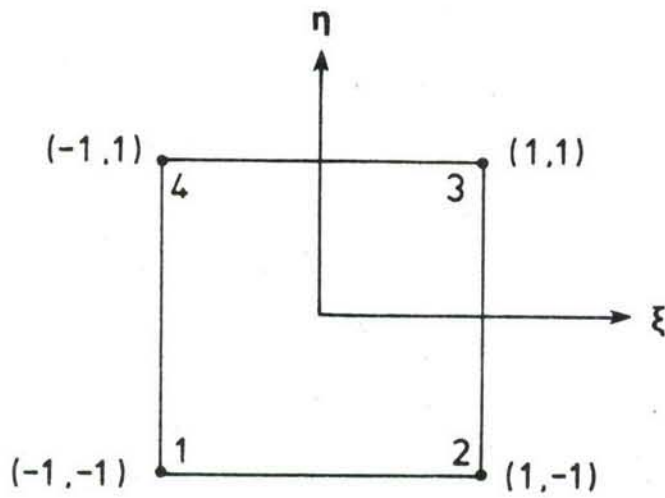
## 2. Quadrilateral Element Formulation

A two-dimensional, four-node element with a general quadrilateral shape is shown in Figure 10(a). In general, the finite element matrices are integrals over the element volume, and the integrations are performed using Gauss quadrature in the  $\xi$ - $\eta$  coordinates shown in Figure 10(b). The element interpolation functions are defined in terms of the natural coordinate variables  $\xi$  and  $\eta$ . Details of the coordinate transformation for conventional interpolation functions are found in Reference 6.

To obtain the nodeless parameter interpolation functions in terms of the natural coordinates  $\xi$  and  $\eta$ , the nodeless parameter interpolation functions for the rectangular element given in Equations 25 and 27 are used. The relations between the local  $x$ - $y$  coordinates (Figure 3) and the  $\xi$ - $\eta$  coordinates (Figure 9b) for the rectangular element are



(a) Global coordinates



(b) Natural coordinates

Figure 10. Four-node isoparametric finite element in global and natural coordinates.

$$\frac{x}{a} = \frac{1}{2} (1 + \xi) \quad (36a)$$

and

$$\frac{y}{b} = \frac{1}{2} (1 + \eta) \quad (36b)$$

With these relations, the element displacement distributions become,

$$u(\xi, \eta) = [N_1 \ N_2 \ N_3 \ N_4] \begin{Bmatrix} u_1 \\ u_2 \\ u_3 \\ u_4 \end{Bmatrix} + [\bar{N}_{u1} \ \bar{N}_{u2} \ \bar{N}_{u3} \ \bar{N}_{u4}] \begin{Bmatrix} T_1 - T_{ref} \\ T_2 - T_{ref} \\ T_3 - T_{ref} \\ T_4 - T_{ref} \end{Bmatrix} \quad (37a)$$

$$v(\xi, \eta) = [N_1 \ N_2 \ N_3 \ N_4] \begin{Bmatrix} v_1 \\ v_2 \\ v_3 \\ v_4 \end{Bmatrix} + [\bar{N}_{v1} \ \bar{N}_{v2} \ \bar{N}_{v3} \ \bar{N}_{v4}] \begin{Bmatrix} T_1 - T_{ref} \\ T_2 - T_{ref} \\ T_3 - T_{ref} \\ T_4 - T_{ref} \end{Bmatrix} \quad (37b)$$

where  $N_i$ ,  $i = 1, 4$  are the conventional bilinear interpolation functions,

$$\begin{aligned} N_1 &= \frac{1}{4} (1 - \xi)(1 - \eta) & N_2 &= \frac{1}{4} (1 + \xi)(1 - \eta) \\ N_3 &= \frac{1}{4} (1 + \xi)(1 + \eta) & N_4 &= \frac{1}{4} (1 - \xi)(1 + \eta) \end{aligned} \quad (38a)$$

and  $\bar{N}_{ui}$  and  $\bar{N}_{vi}$ ,  $i = 1, 4$ , are the nodeless parameter interpolation functions corresponding to the  $u$ - and  $v$ -displacements, respectively,

$$\bar{N}_{u1} = \frac{\alpha}{16} a(1-\xi^2)(1-n) \quad \bar{N}_{u2} = -\frac{\alpha}{16} a(1-\xi^2)(1-n) \quad (38b)$$

$$\bar{N}_{u3} = -\frac{\alpha}{16} a(1-\xi^2)(1+n) \quad \bar{N}_{u4} = \frac{\alpha}{16} a(1-\xi^2)(1+n)$$

$$\bar{N}_{v1} = \frac{\alpha}{16} b(1-\xi)(1-n^2) \quad \bar{N}_{v2} = \frac{\alpha}{16} b(1+\xi)(1-n^2) \quad (38c)$$

$$\bar{N}_{v3} = -\frac{\alpha}{16} b(1+\xi)(1-n^2) \quad \bar{N}_{v4} = -\frac{\alpha}{16} b(1-\xi)(1-n^2)$$

Note that these nodeless parameter interpolation functions depend on the coefficient of thermal expansion, the dimensions of the element and the natural coordinates  $\xi$  and  $n$ .

For an element with general quadrilateral shape, it is not possible to derive the nodeless parameter interpolation functions as for the rectangular element given by Equations 38b-c. However, the nodeless parameter interpolation functions obtained for rectangular element can be modified and used approximately for the quadrilateral element in the following forms,

$$\bar{N}_{u1} = \frac{\alpha}{16} \ell_{12} (1-\xi^2)(1-n) \quad \bar{N}_{u2} = -\frac{\alpha}{16} \ell_{12} (1-\xi^2)(1-n) \quad (39a)$$

$$\bar{N}_{u3} = -\frac{\alpha}{16} \ell_{34} (1-\xi^2)(1+n) \quad \bar{N}_{u4} = \frac{\alpha}{16} \ell_{34} (1-\xi^2)(1+n)$$

$$\bar{N}_{v1} = \frac{\alpha}{16} l_{41} (1-\xi)(1-\eta^2) \quad \bar{N}_{v2} = \frac{\alpha}{16} l_{23} (1+\xi)(1-\eta^2) \quad (39b)$$

$$\bar{N}_{v3} = -\frac{\alpha}{16} l_{23} (1+\xi)(1-\eta^2) \quad \bar{N}_{v4} = -\frac{\alpha}{16} l_{41} (1-\xi)(1-\eta^2)$$

where  $l_{ij}$ ,  $i, j = 1, 4$ , are the lengths of the element edges between nodes  $i$  and  $j$ . With the above nodeless interpolation functions, the element displacement distributions given by Equation 37 are shown in Figure 11.

### 3. Hexahedral Element Formulation

Figure 12 shows an eight-node hexahedral element in both global and natural coordinates. In the thermal analysis, the conventional element temperature distribution ( $P_T = 1$ ) is expressed in terms of the natural coordinates  $\xi$ ,  $\eta$  and  $\zeta$  in the form (Reference 6),

$$T(\xi, \eta, \zeta, t) = [N_T(\xi, \eta, \zeta)] \{T(t)\} = \sum_{i=1}^8 N_i T_i \quad (40)$$

where  $N_i$ ,  $i=1, 8$ , are the element temperature interpolation functions given by

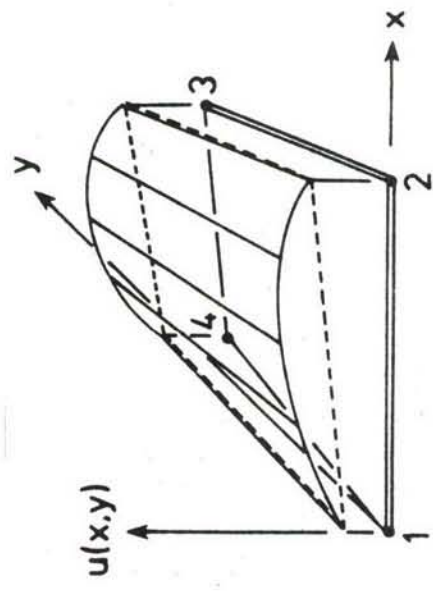
$$N_i = \frac{1}{8} (1 + \xi \xi_i)(1 + \eta \eta_i)(1 + \zeta \zeta_i) \quad (41)$$

and  $T_i$  are the element nodal temperatures which may be a function of time  $t$ .

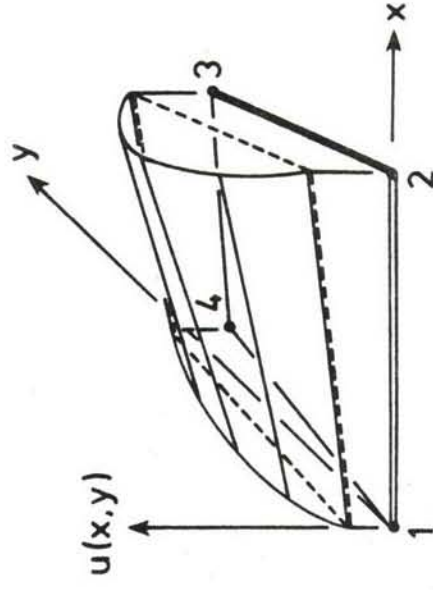
The congruent structural element at each node has three displacement unknowns,  $u$ ,  $v$ , and  $w$  in the directions of the element local coordin-

----- Conventional, bilinear, 4-node element

—— Quadratic, 4-node element with nodeless parameters

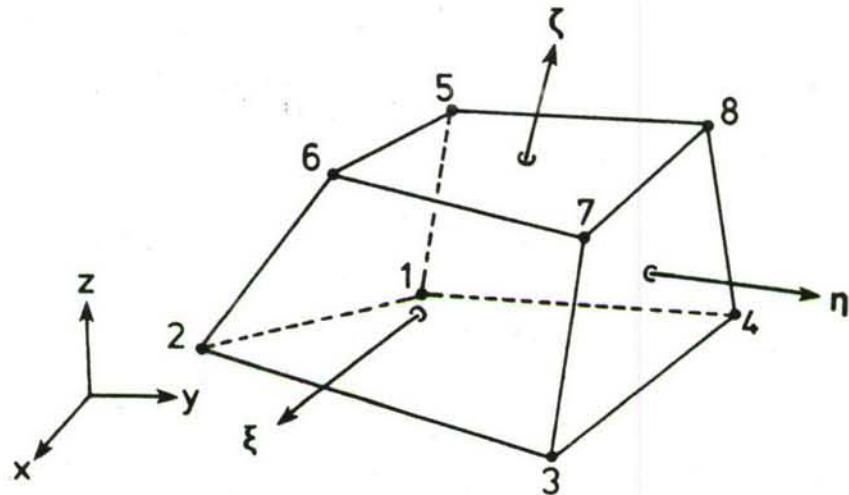


(a)

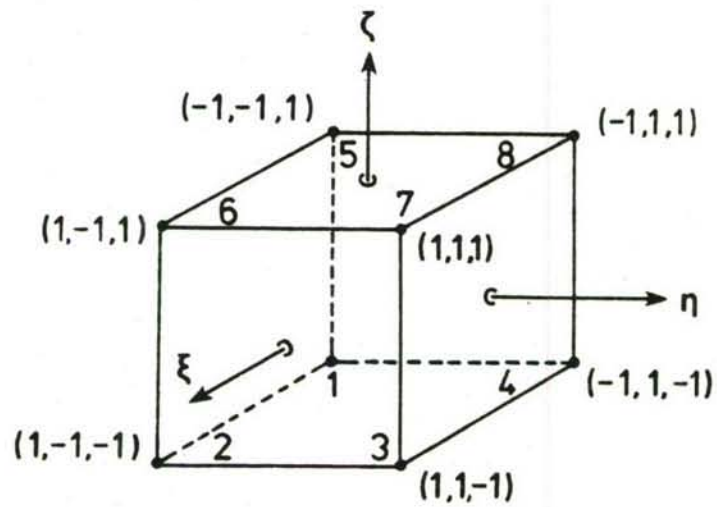


(b)

Figure 11. Quadrilateral structural element displacement distributions.



(a) Global coordinates



(b) Natural coordinates

Figure 12. Eight-node isoparametric finite element in global and natural coordinates.

ates  $x$ ,  $y$  and  $z$ , respectively. The nodeless parameter structural element can be constructed by first writing the three displacement distributions in the following forms,

$$u = [N_S] \{u\} + [\bar{N}_u] \{T - T_{ref}\} \quad (42a)$$

$$v = [N_S] \{v\} + [\bar{N}_v] \{T - T_{ref}\} \quad (42b)$$

and

$$w = [N_S] \{w\} + [\bar{N}_w] \{T - T_{ref}\} \quad (42c)$$

where  $[N_S]$  is the row matrix of the conventional displacement interpolation functions given by Equation 41.  $[\bar{N}_u]$ ,  $[\bar{N}_v]$  and  $[\bar{N}_w]$  are the nodeless interpolation matrices to be determined, and  $\{T\}$  is the vector of element nodal temperatures shown in Equation 40.

To determine the nodeless interpolation functions, the procedures described in sections IV.1 and IV.2 are employed. Using the assumed element displacement distributions in the form of Equation 42, the element strain-displacement and stress-strain relations are formulated. To reduce the element stress discontinuity, the strains associated with the nodeless parameter interpolation functions are forced to have the same algebraic order as the thermal strains. These conditions and the element boundary conditions required to preserve the element displacement continuity lead to the determination of the unknown nodeless parameter interpolation functions. The nodeless parameter interpolation functions corresponding to the  $u$ ,  $v$  and

w displacements are:

$$\bar{N}_{u1} = -\bar{N}_{u2} = \frac{\alpha}{32} \ell_{12} (1-\xi^2)(1-\eta)(1-\zeta)$$

$$\bar{N}_{u3} = -\bar{N}_{u4} = -\frac{\alpha}{32} \ell_{34} (1-\xi^2)(1+\eta)(1-\zeta)$$

(43a)

$$\bar{N}_{u5} = -\bar{N}_{u6} = \frac{\alpha}{32} \ell_{56} (1-\xi^2)(1-\eta)(1+\zeta)$$

$$\bar{N}_{u7} = -\bar{N}_{u8} = -\frac{\alpha}{32} \ell_{78} (1-\xi^2)(1+\eta)(1+\zeta)$$

$$\bar{N}_{v1} = -\bar{N}_{v4} = \frac{\alpha}{32} \ell_{14} (1-\xi)(1-\eta^2)(1-\zeta)$$

$$\bar{N}_{v2} = -\bar{N}_{v3} = \frac{\alpha}{32} \ell_{23} (1+\xi)(1-\eta^2)(1-\zeta)$$

(43b)

$$\bar{N}_{v5} = -\bar{N}_{v8} = \frac{\alpha}{32} \ell_{58} (1-\xi)(1-\eta^2)(1+\zeta)$$

$$\bar{N}_{v6} = -\bar{N}_{v7} = \frac{\alpha}{32} \ell_{67} (1+\xi)(1-\eta^2)(1+\zeta)$$

$$\begin{aligned}
\bar{N}_{w1} = -\bar{N}_{w5} &= \frac{\alpha}{32} \ell_{15} (1-\xi)(1-\eta)(1-\zeta^2) \\
\bar{N}_{w2} = -\bar{N}_{w6} &= \frac{\alpha}{32} \ell_{26} (1+\xi)(1-\eta)(1-\zeta^2) \\
\bar{N}_{w3} = -\bar{N}_{w7} &= \frac{\alpha}{32} \ell_{37} (1+\xi)(1+\eta)(1-\zeta^2) \\
\bar{N}_{w4} = -\bar{N}_{w8} &= \frac{\alpha}{32} \ell_{48} (1-\xi)(1+\eta)(1-\zeta^2)
\end{aligned}
\tag{43c}$$

where  $\ell_{ij}$ ,  $i, j = 1, 8$ , are the length of element edges between nodes  $i$  and  $j$ .

Element matrices can be derived as described in section IV.1.2 and the element equations are obtained in the form of Equation 33. Since each node has three displacement components, there are 24 unknowns for an element which is equal to the number of unknowns used in the conventional 8-node element. After the nodal displacement components are computed, the element displacement distributions and the element stresses are obtained using Equations 42 and 35, respectively.

#### 4. Formulation for Quadratic Temperature Distribution

In the thermal analysis, a two-dimensional element with quadratic temperature distribution can be constructed using the hierarchical approach. As described in Section III.3, the hierarchical element temperature distribution ( $P_T = 2$ ) is expressed in the form,

$$T = [N_1 \quad N_2 \quad N_3 \quad N_4] \begin{Bmatrix} T_1 \\ T_2 \\ T_3 \\ T_4 \end{Bmatrix} + [N_5 \quad N_6 \quad N_7 \quad N_8] \begin{Bmatrix} T_5 \\ T_6 \\ T_7 \\ T_8 \end{Bmatrix} \quad (44)$$

where  $T_i$ ,  $i = 1,4$  are the element nodal temperatures and  $T_i$ ,  $i = 5,8$  are the nodeless variables. For a rectangular element, the element interpolation functions  $N_i$ ,  $i = 1,4$  are the same as for the conventional bilinear four-node element given in Equation 2. The interpolation functions  $N_i$ ,  $i = 5,8$  for the nodeless variables are given by,

$$\begin{aligned} N_5 &= 4 \frac{x}{a} \left(1 - \frac{x}{a}\right) \left(1 - \frac{y}{b}\right) & N_6 &= 4 \frac{x}{a} \frac{y}{b} \left(1 - \frac{y}{b}\right) \\ N_7 &= 4 \frac{x}{a} \left(1 - \frac{x}{a}\right) \frac{y}{b} & N_8 &= 4 \left(1 - \frac{x}{a}\right) \frac{y}{b} \left(1 - \frac{y}{b}\right) \end{aligned} \quad (45)$$

To formulate a nodeless parameter structural element for the quadratic temperature distribution, the procedures described in Section IV.1.1 are employed. The structural element displacement distributions are first written as the combination of the bilinear distribution and the distribution associated with the element temperature,

$$u = [N_1 \quad N_2 \quad N_3 \quad N_4] \begin{Bmatrix} u_1 \\ u_2 \\ u_3 \\ u_4 \end{Bmatrix} + [\bar{N}_{u1} \quad \bar{N}_{u2} \quad \bar{N}_{u3} \quad \bar{N}_{u4} \quad \bar{N}_{u5} \quad \bar{N}_{u6} \quad \bar{N}_{u7} \quad \bar{N}_{u8}] \begin{Bmatrix} T_1 - T_{ref} \\ T_2 - T_{ref} \\ T_3 - T_{ref} \\ T_4 - T_{ref} \\ T_5 \\ T_6 \\ T_7 \\ T_8 \end{Bmatrix} \quad (46)$$

$$v = [N_1 \quad N_2 \quad N_3 \quad N_4] \begin{Bmatrix} v_1 \\ v_2 \\ v_3 \\ v_4 \end{Bmatrix} + [\bar{N}_{v1} \quad \bar{N}_{v2} \quad \bar{N}_{v3} \quad \bar{N}_{v4} \quad \bar{N}_{v5} \quad \bar{N}_{v6} \quad \bar{N}_{v7} \quad \bar{N}_{v8}] \begin{Bmatrix} T_1 - T_{ref} \\ T_2 - T_{ref} \\ T_3 - T_{ref} \\ T_4 - T_{ref} \\ T_5 \\ T_6 \\ T_7 \\ T_8 \end{Bmatrix}$$

where  $\bar{N}_{u_i}$  and  $\bar{N}_{v_i}$ ,  $i = 1,8$  are the nodeless parameter interpolation functions to be determined. The strain-displacement and the stress-strain relations shown in Equations 18 and 19 are then formulated. To reduce the stress discontinuity between elements, the strains produced by the nodeless parameter displacement distributions are forced to have the same order as the thermal strains. As an example for plane stress, this requirement for the  $u$  displacement yields

$$\left[ \begin{array}{cccccccc} \frac{\partial \bar{N}_{u1}}{\partial x} & \frac{\partial \bar{N}_{u2}}{\partial x} & \frac{\partial \bar{N}_{u3}}{\partial x} & \frac{\partial \bar{N}_{u4}}{\partial x} & \frac{\partial \bar{N}_{u5}}{\partial x} & \frac{\partial \bar{N}_{u6}}{\partial x} & \frac{\partial \bar{N}_{u7}}{\partial x} & \frac{\partial \bar{N}_{u8}}{\partial x} \end{array} \right] \left\{ \begin{array}{l} T_1 - T_{ref} \\ T_2 - T_{ref} \\ T_3 - T_{ref} \\ T_4 - T_{ref} \\ T_5 \\ T_6 \\ T_7 \\ T_8 \end{array} \right\}$$

$$= \alpha \left[ \left(1 - \frac{x}{a}\right)\left(1 - \frac{y}{b}\right) \quad \frac{x}{a} \left(1 - \frac{y}{b}\right) \quad \frac{x}{a} \frac{y}{b} \quad \left(1 - \frac{x}{a}\right) \frac{y}{b} \quad 4 \frac{x}{a} \left(1 - \frac{x}{a}\right) \left(1 - \frac{y}{b}\right) \right.$$

$$\left. 4 \frac{x}{a} \frac{y}{b} \left(1 - \frac{y}{b}\right) \quad 4 \frac{x}{a} \left(1 - \frac{x}{a}\right) \frac{y}{b} \quad 4 \left(1 - \frac{x}{a}\right) \frac{y}{b} \quad \left(1 - \frac{y}{b}\right) \right] \left\{ \begin{array}{l} T_1 - T_{ref} \\ T_2 - T_{ref} \\ T_3 - T_{ref} \\ T_4 - T_{ref} \\ T_5 \\ T_6 \\ T_7 \\ T_8 \end{array} \right\}$$

$$+ [ a_1 \quad b_1 \quad c_1 \quad d_1 \quad e_1 \quad f_1 \quad g_1 \quad h_1 ] \left\{ \begin{array}{l} T_1 - T_{ref} \\ T_2 - T_{ref} \\ T_3 - T_{ref} \\ T_4 - T_{ref} \\ T_5 \\ T_6 \\ T_7 \\ T_8 \end{array} \right\} \quad (47)$$

where the coefficients in the row matrix of the second term on the right hand side of the equation are constants. Using the method of undetermined coefficients and imposing the conditions of displacement continuity requirement between elements, the unknown nodeless parameter interpolation functions  $\bar{N}_{ui}$ ,  $i = 1,8$  are determined. The nodeless parameter interpolation functions corresponding to the  $u$  and  $v$  displacements are,

$$\bar{N}_{u1} = -\bar{N}_{u2} = \frac{\alpha}{2} \left( x - \frac{x^2}{a} \right) \left( 1 - \frac{y}{b} \right)$$

$$\bar{N}_{u3} = -\bar{N}_{u4} = -\frac{\alpha}{2} \left( x - \frac{x^2}{a} \right) \frac{y}{b}$$

$$\bar{N}_{u5} = 4\alpha \left( -\frac{x}{6} + \frac{x^2}{2a} - \frac{x^3}{3a^2} \right) \left( 1 - \frac{y}{b} \right)$$

$$\bar{N}_{u6} = 4\alpha \left( -\frac{x}{2} + \frac{x^2}{2a} \right) \frac{y}{b} \left( 1 - \frac{y}{b} \right)$$

$$\bar{N}_{u7} = 4\alpha \left( -\frac{x}{6} + \frac{x^2}{2a} - \frac{x^3}{3a^2} \right) \frac{y}{b}$$

$$\bar{N}_{u8} = 4\alpha \left( \frac{x}{2} - \frac{x^2}{2a} \right) \frac{y}{b} \left( 1 - \frac{y}{b} \right)$$

$$\bar{N}_{v1} = -\bar{N}_{v4} = \frac{\alpha}{2} \left(1 - \frac{x}{a}\right) \left(y - \frac{y^2}{b}\right)$$

$$\bar{N}_{v2} = -\bar{N}_{v3} = \frac{\alpha}{2} \frac{x}{a} \left(y - \frac{y^2}{b}\right)$$

$$\bar{N}_{v5} = 4\alpha \frac{x}{a} \left(1 - \frac{x}{a}\right) \left(\frac{y}{2} - \frac{y^2}{2b}\right)$$

$$\bar{N}_{v6} = 4\alpha \frac{x}{a} \left(-\frac{y}{6} + \frac{y^2}{2b} - \frac{y^3}{3b^2}\right)$$

$$\bar{N}_{v7} = 4\alpha \frac{x}{a} \left(1 - \frac{x}{a}\right) \left(-\frac{y}{2} + \frac{y^2}{2b}\right)$$

$$\bar{N}_{v8} = 4\alpha \left(1 - \frac{x}{a}\right) \left(-\frac{y}{6} + \frac{y^2}{2b} - \frac{y^3}{3b^2}\right)$$

## 5. Comments on Formulation

For the two-dimensional element described in Section IV.1, the nodeless parameter interpolation functions were obtained for a rectangular element. For a general quadrilateral element, the nodeless parameter interpolation functions do not appear to be derived easily. The nodeless parameter interpolation functions for rectangular element were modified and used approximately for a quadrilateral element. For this reason, the quadrilateral nodeless parameter element (Equations 37-39) will provide maximum performance if the element shape is close to rectangular.

Figure 9 shows that the nodeless parameter interpolation functions are not geometrically isotropic; the functions depend on the element orientation. This means that care must be taken in element nodal numbering to ensure compatibility of displacements at element interfaces. This lack of geometric isotropy restricts the generality of the element formulation. The element displacement and stress distributions compared to the conventional element solutions may not be improved when this situation occurs and further investigation is required to evaluate the element performance under these conditions.

SECTION V  
APPLICATIONS

To demonstrate the capabilities of the hierarchical and the nodeless parameter finite elements described in Sections III and IV, four thermal-stress problems are analyzed: (1) a free expansion plate with linear temperature distribution, (2) a fixed end beam with quadratic temperature distribution through the beam depth, (3) a simplified wing section with aerodynamic heating, and (4) a convectively cooled laser mirror. In each problem, benefits of utilizing the hierarchical and nodeless parameter finite elements are demonstrated by comparison with results from conventional finite elements and, where possible, analytical solutions.

1. Free Expansion Plate with Linear Temperature Distribution

Both hierarchical and nodeless parameter finite elements are used for the structural analysis of the free expansion plate with linear temperature distribution (Figure 4(a)) as described previously in Section II.3. The plate is modeled by: (1) one conventional finite element, (2) one nodeless parameter finite element, and (3) one hierarchical finite element ( $P_S = 2$ ). To illustrate the performance of these finite elements, the analytical solutions for displacements and stresses were derived. Since the plate is subjected to a linear temperature distribution and is free to expand, all stress components are zero. With the linear temperature distribution in the x-direction, the analytical solution for the displacement are:

$$u = \alpha x T_1 + \frac{\alpha}{2a} (x^2 - y^2) (T_2 - T_1) \quad (48a)$$

and 
$$v = \alpha y T_1 + \frac{\alpha}{a} xy (T_2 - T_1) \quad (48b)$$

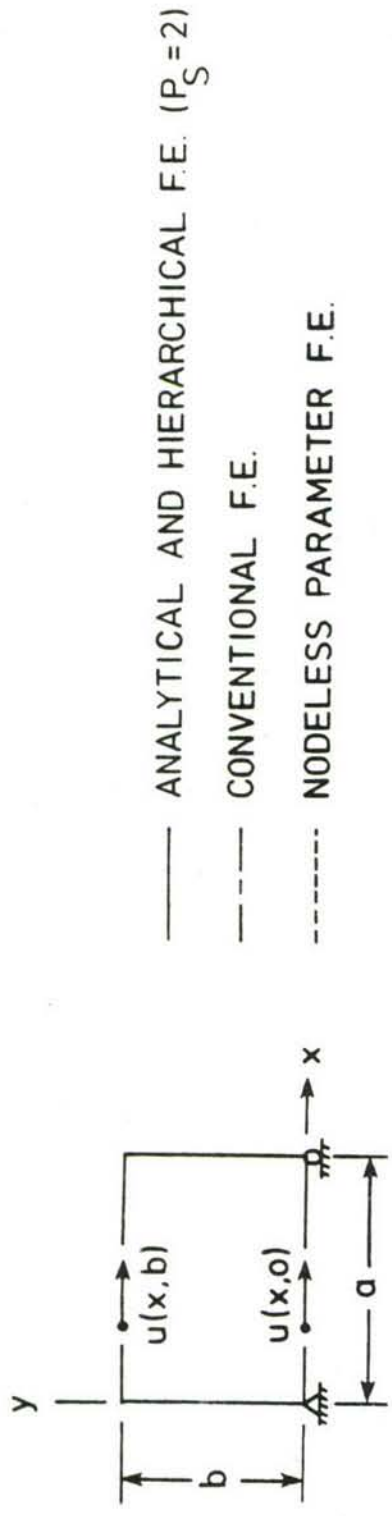
where  $\alpha$  is the thermal expansion coefficient of the plate;  $T_1$  and  $T_2$  are the temperatures along the edges  $x = 0$  and  $x = a$ , respectively.

Figure 13 shows the comparative  $u$ -displacement distributions for the analytical solution and the three finite element solutions along the edges  $y = 0$  and  $y = b$ . Since the hierarchical element with  $P_S = 2$  uses quadratic displacement distributions, the displacement solutions obtained are exact. At  $y = 0$  the computed nodal  $u$ -displacement at  $x = a$  from all three finite element models are exact; however, the conventional finite element is unable to provide a realistic displacement distribution for  $0 < x < a$ . Similarly, along edge  $y = b$ , the conventional finite element solution tends to average the true displacement distribution whereas the nodeless parameter element gives excellent agreement with the exact solution.

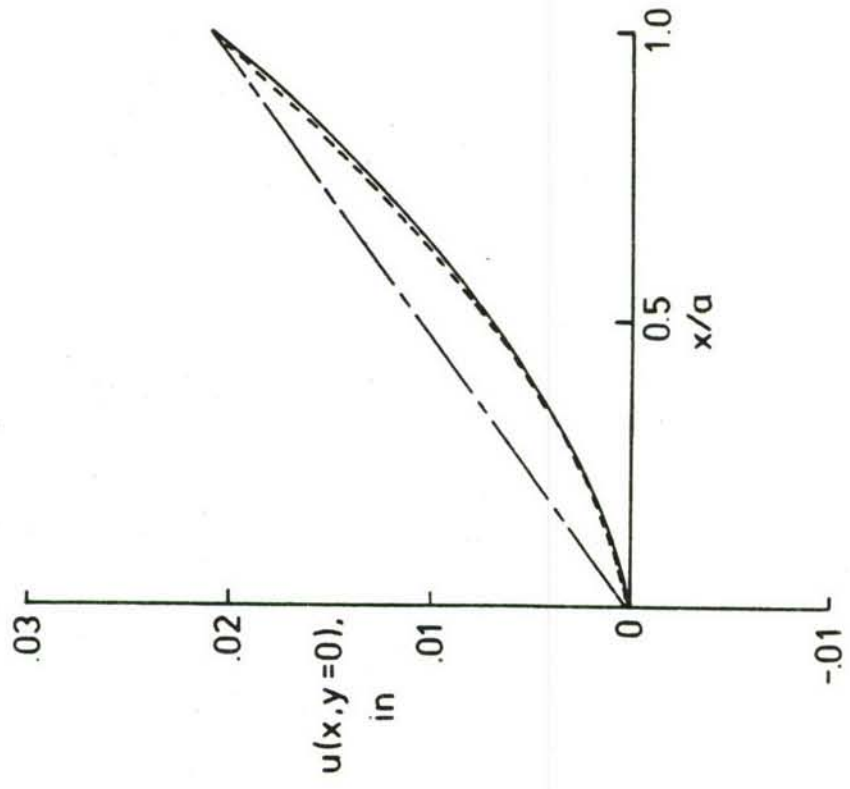
Element stress distributions  $\sigma_x$  along the edge  $y = 0$  and  $\sigma_y$  along the edge  $x = 0$  obtained from the three finite element models are shown in Figure 14(a) and (b), respectively. The hierarchical element provides exact zero stresses throughout the plate. Due to the linear temperature distribution in the  $x$ -direction, an unrealistic distribution for  $\sigma_x$  is obtained from the conventional element. The nodeless parameter element improves this stress distribution significantly and clearly demonstrates the capability of providing more realistic stress distributions.

## 2. Fixed End Beam with Quadratic Temperature Distribution

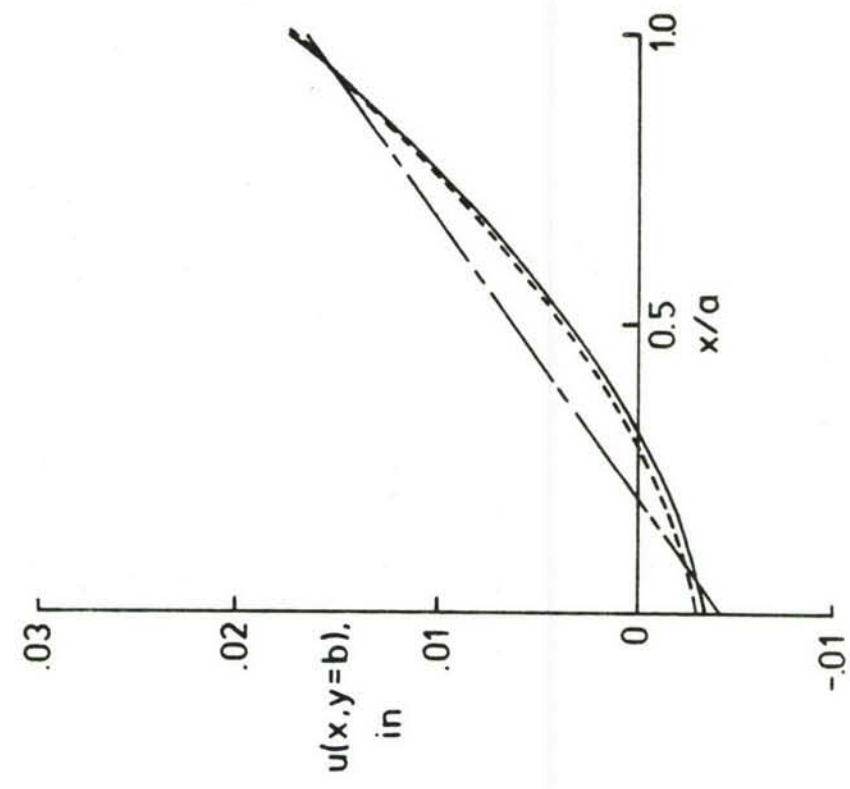
A beam with a symmetrical quadratic temperature distribution through



- ANALYTICAL AND HIERARCHICAL F.E. ( $P_S=2$ )
- - - CONVENTIONAL F.E.
- - - NODELESS PARAMETER F.E.

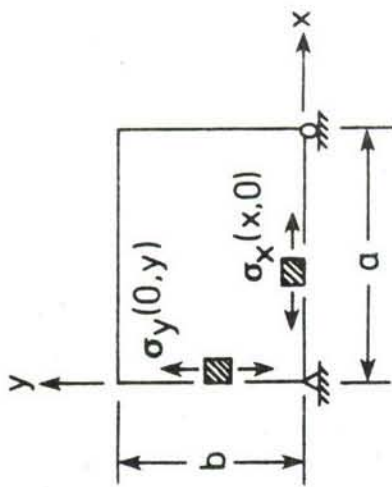


(a)



(b)

Figure 13. Comparative displacement distributions for a free expansion plate with linear temperature distribution.



- ANALYTICAL AND HIERARCHICAL F.E. ( $P_S=2$ )
- - - CONVENTIONAL F.E.
- - - NODELESS PARAMETER F.E.

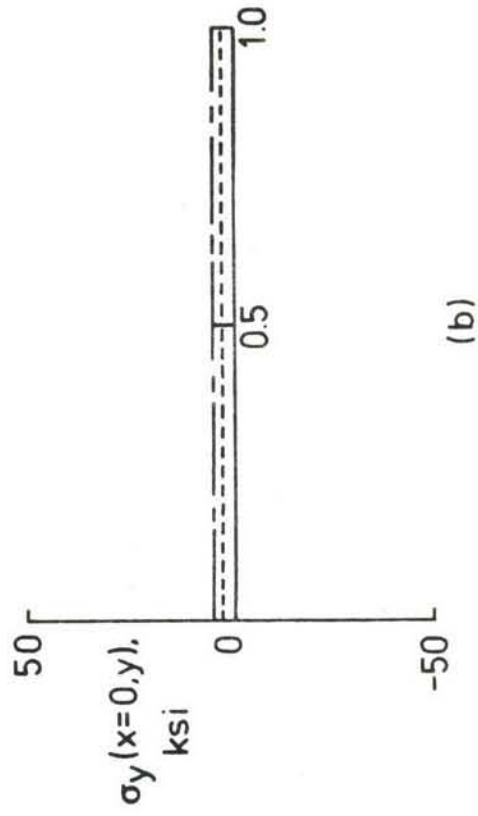
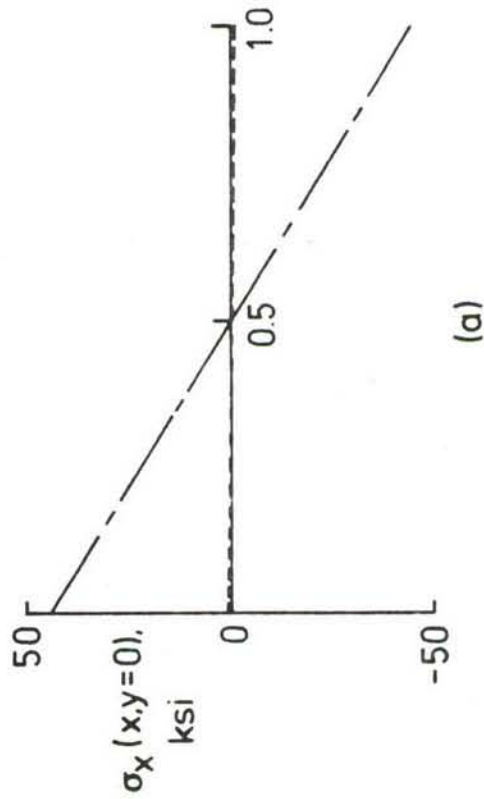


Figure 14. Comparative thermal stress distributions for a free expansion plate with linear temperature distribution.

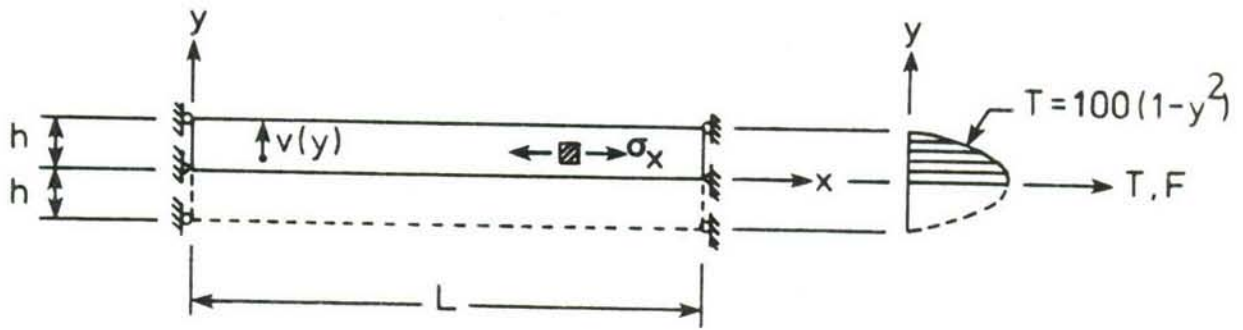
its depth is shown in Figure 15(a). The beam is fixed in the longitudinal direction at both ends but is free to move in the transverse direction due to the constraints  $u = 0$  and  $v = v(y)$ . Using symmetry, the upper half of the beam is modeled by: (1) one conventional element, and (2) one nodeless parameter element.

Figure 15(b) shows the comparative transverse displacement distributions from an analytical solution (Reference 11), the conventional element and the nodeless parameter element solutions. The conventional element gives a relatively high error for both the nodal displacement and the displacement distribution. The nodeless parameter element yields the exact nodal displacement and gives an excellent representation of the displacement distribution.

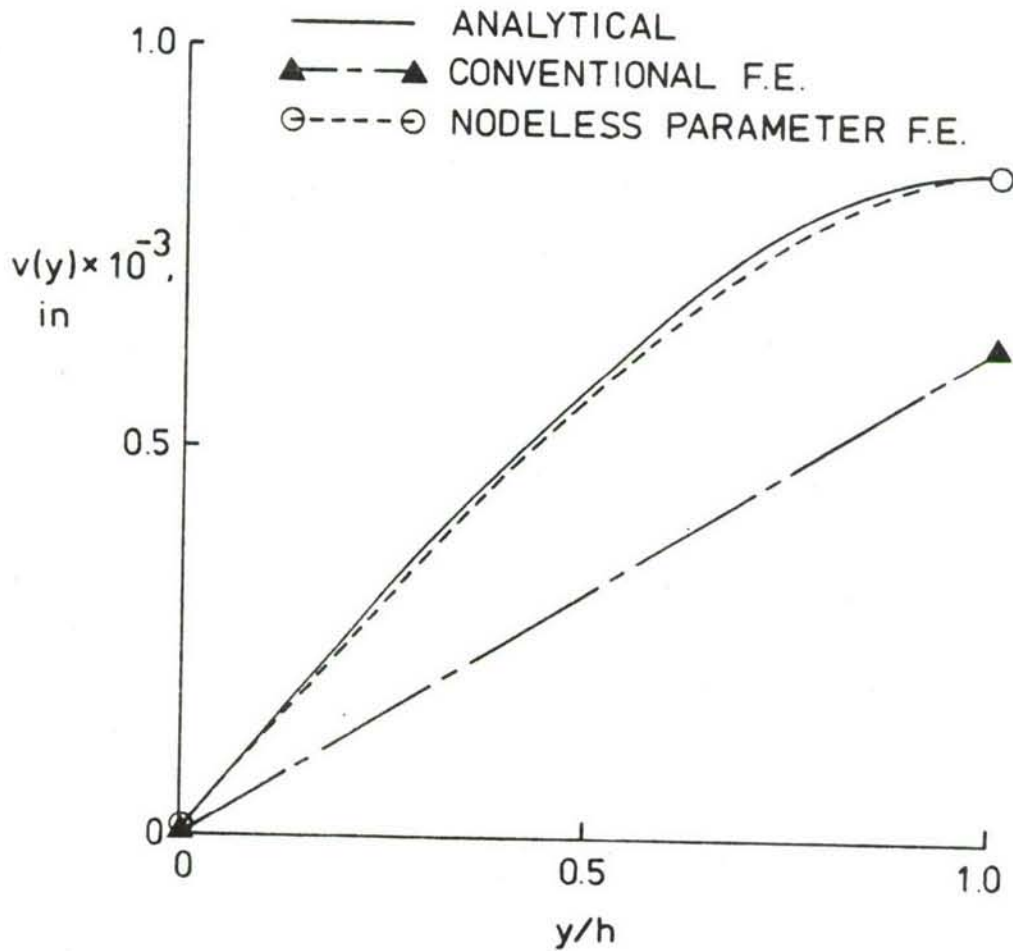
The stress distributions obtained from these finite element models are compared with the analytical solution in Figure 15(c). The element stress distribution predicted by the nodeless parameter element is in very good agreement with the analytical solution. The conventional element is unable to provide details of the nonuniform stress distribution. As mentioned earlier, element centroidal stresses are not the correct estimates of the true stresses in general. This phenomenon is clearly shown by this example where the centroidal stress obtained from the conventional elements is underestimated significantly.

### 3. Simplified Wing Section with Aerodynamic Heating

A simplified wing section (Figure 16a) consisting of metallic top and bottom skins connected by corrugated spars is subjected to symmetrical, non-uniform step-function representations of time-dependent aerodynamic heating. The finite element discretization is based on a unit length of the wing sec-

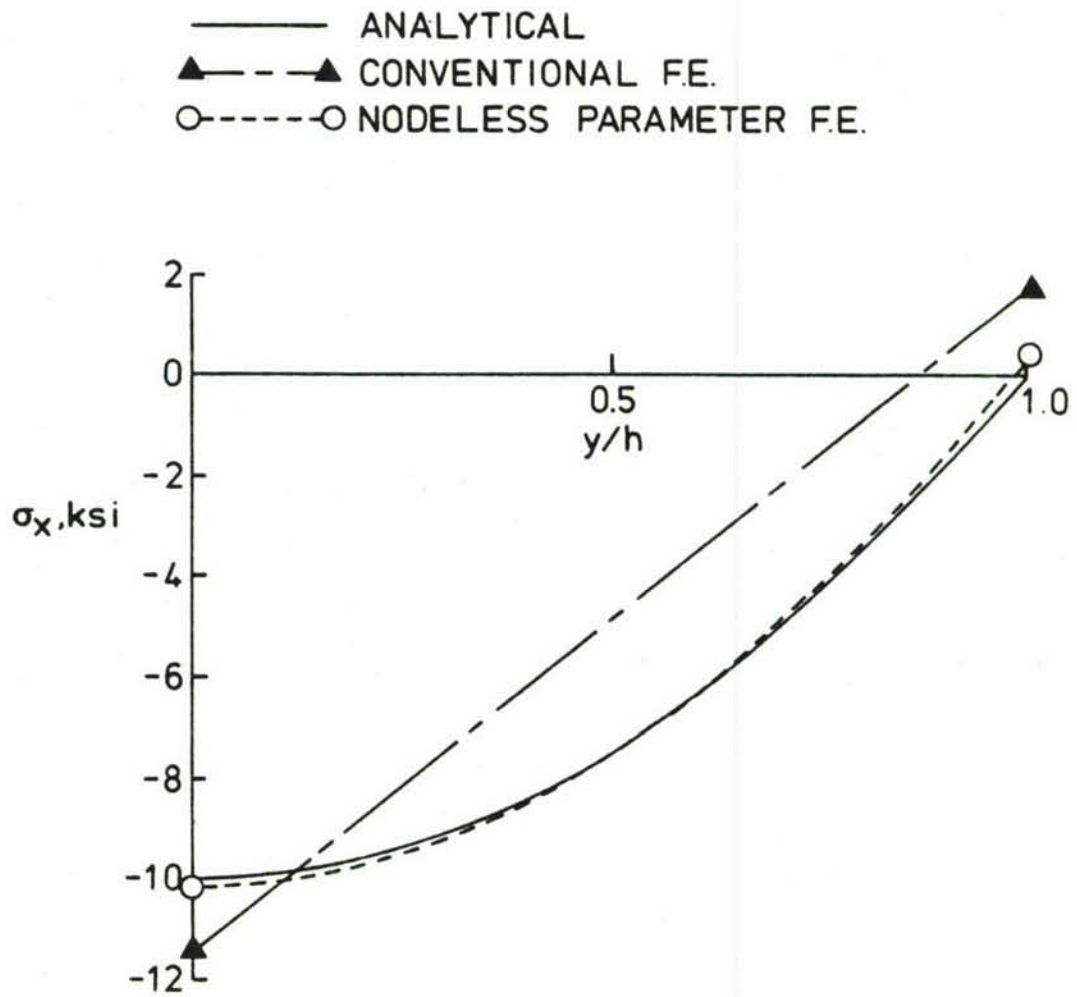


(a) Fixed end beam with nonlinear temperature distribution.



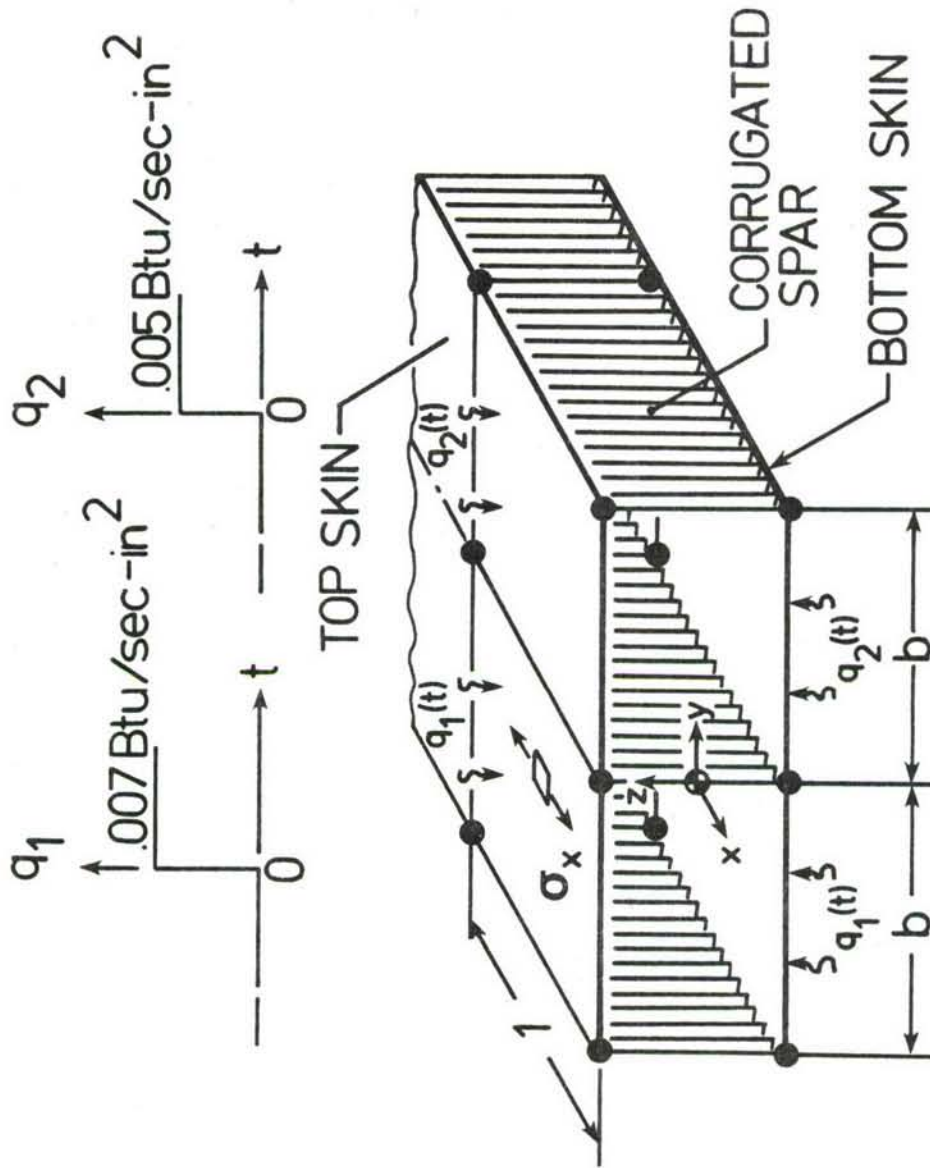
(b) Comparative transverse displacement distributions.

Figure 15. Conventional and nodeless parameter finite element solutions for a fixed end beam with nonlinear temperature distribution.



(c) Comparative thermal stress distributions.

Figure 15. Concluded.



### (a) SIMPLIFIED WING SECTION WITH AERODYNAMIC HEATING

Figure 16. Hierarchical thermal-structural analysis of simplified wing section with aerodynamic heating.

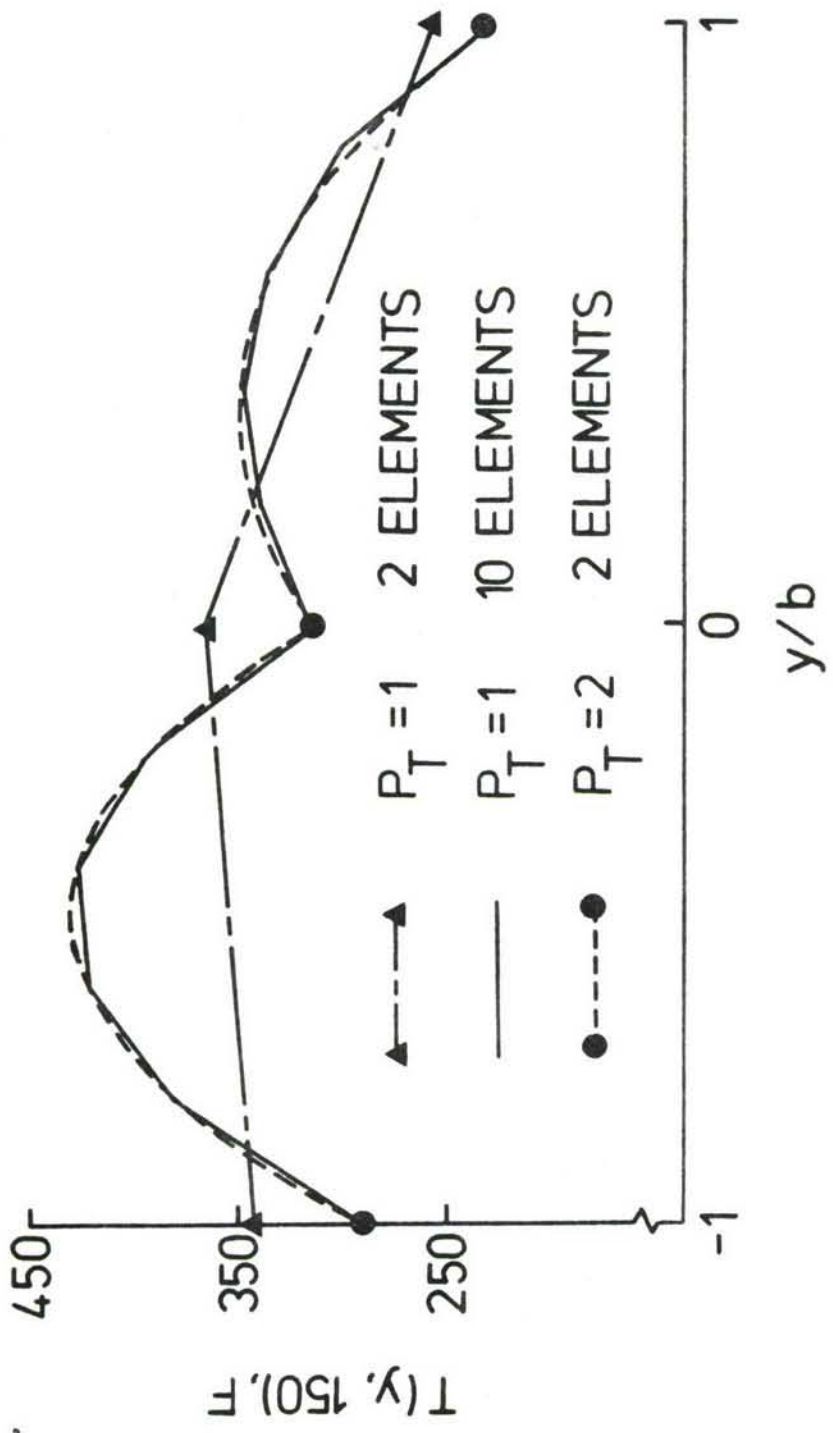
tion and models a one-dimensional transverse variation of temperature and thermal stress. Three finite element models were used for the analyses. The first model consists of seven linear elements ( $P_T = P_S = 1$ ); two elements each for the top and bottom skins and one element for each spar. The second model used a refined mesh with ten linear elements for each skin. The third model is identical to the first model except quadratic hierarchical interpolation functions were employed for the thermal analysis ( $P_T = 2$ ) and linear interpolation functions ( $P_S = 1$ ) were employed for the structural analysis. The comparative corresponding skin temperatures at  $t = 150$  s. are shown in Figure 16b, and the corresponding skin thermal stresses are shown in Figure 16c.

For both temperature and stress, the hierarchical approach with  $P_T = 2$  and  $P_S = 1$  predicts realistic solutions and gives good agreement with the results from the refined mesh of linear elements. The first model with linear elements is unable to represent the nonuniform temperature and stress distributions. But with the same discretization, the addition of the quadratic interpolation functions for the temperature is clearly sufficient to resolve the pertinent details of both the thermal and structural solutions.

#### 4. Convectively Cooled Laser Mirror

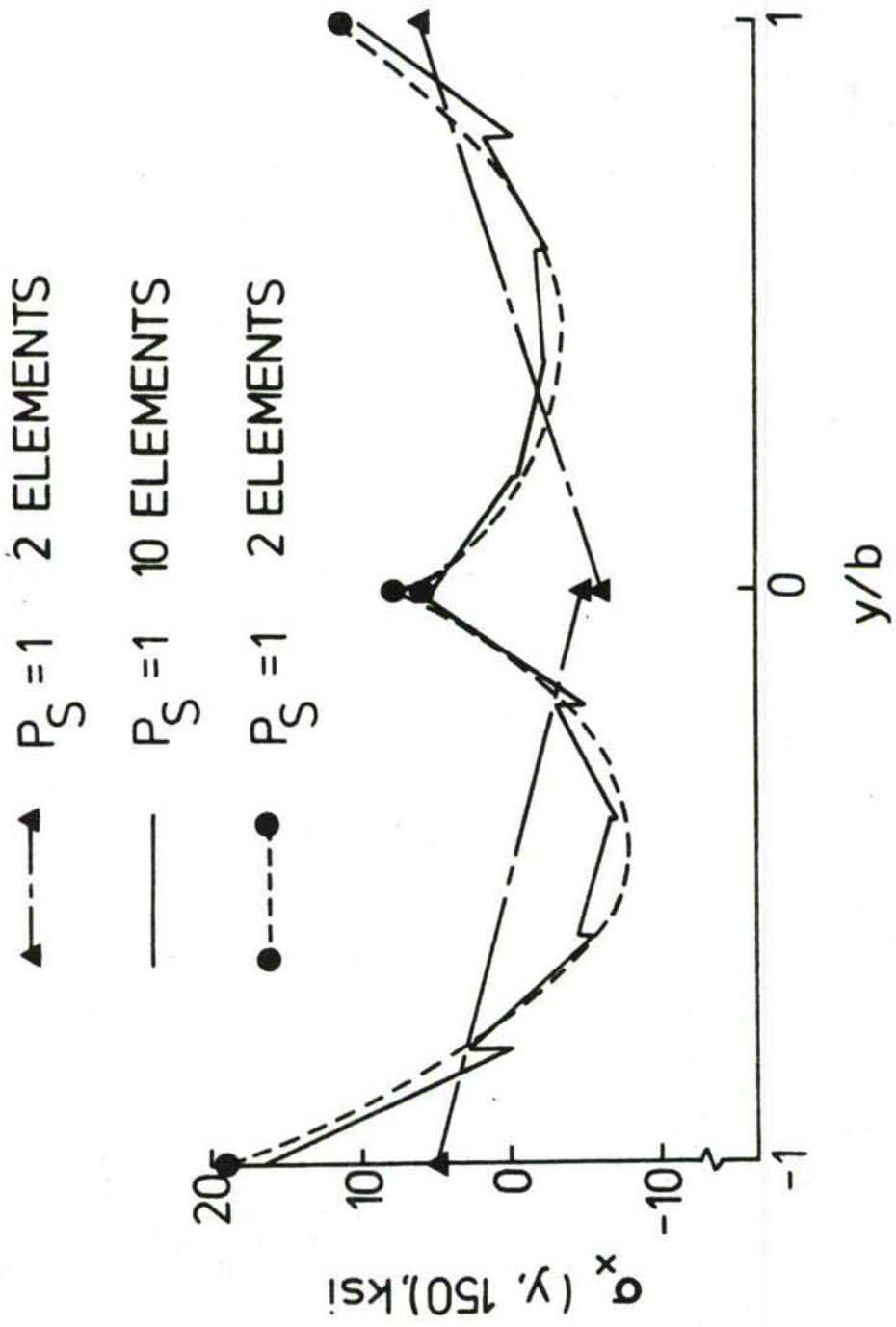
Figure 17(a) illustrates a design concept of a convectively cooled laser mirror. The mirror is subjected to high uniform specified surface heating. To reduce stresses and deformations, the mirror is convectively cooled by flow through multiple coolant passages. Using symmetry, the finite element discretization shown in Figure 17(b) was established for a preliminary thermal-stress analysis.

The thermal analysis was simplified by using a two dimensional model of

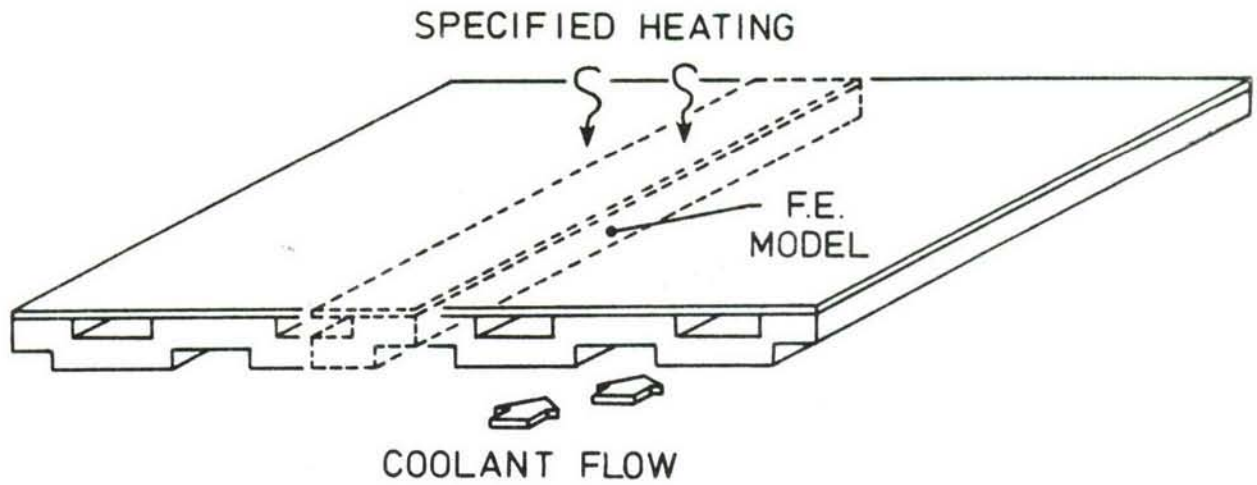


(b) COMPARATIVE TEMPERATURE DISTRIBUTIONS ALONG CHORDWISE DIRECTION,  $t = 150$  sec.

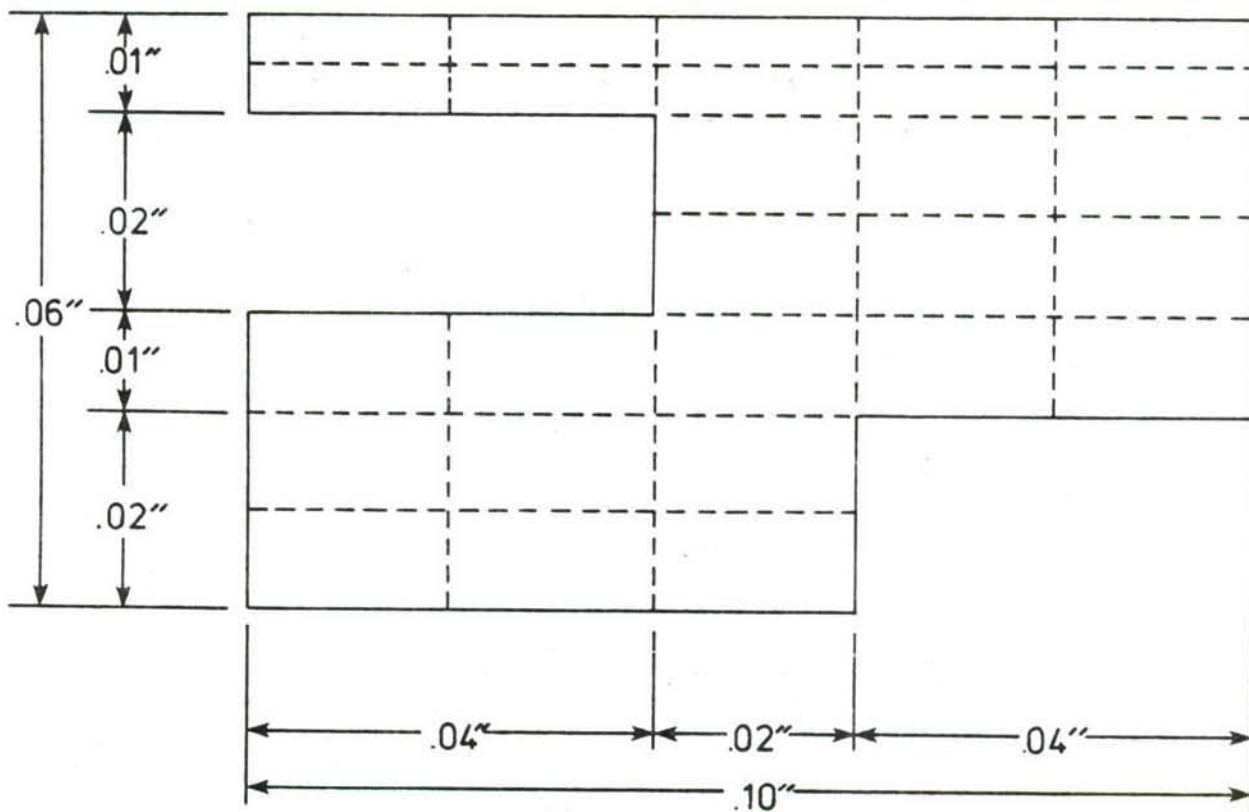
Figure 16. Continued.



(c) COMPARATIVE THERMAL STRESS DISTRIBUTIONS ALONG CHORDWISE DIRECTION,  $t=150$  sec.



(a) CONVECTIVELY COOLED LASER MIRROR



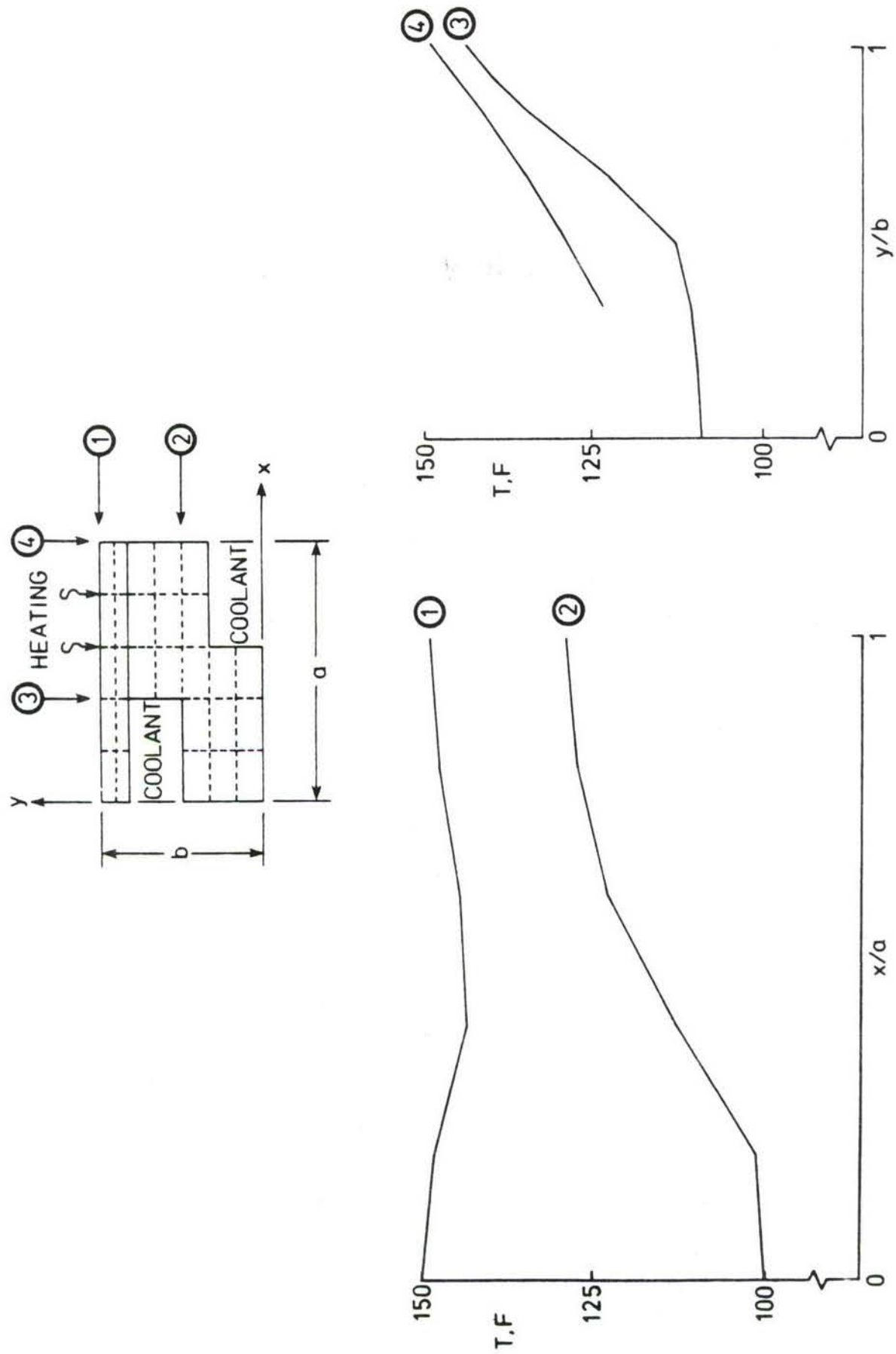
(b) FINITE ELEMENT MODEL

Figure 17. Thermal-structural analysis of convectively cooled laser mirror.

a mirror cross-section with specified coolant temperature. Steady-state conduction with convection heat transfer to the coolant was analyzed. The bottom mirror surface was assumed to be adiabatic, and the left and right edges of the mirror have zero heat transfer by symmetry. Conventional bilinear thermal elements ( $P_T = 1$ ) were used in the analysis. Temperature distributions at four sections through the mirror are shown in Figure 18. Since the temperatures obtained are relatively smooth, the conventional bilinear element model for the thermal analysis was sufficient and no additional refinement was required.

For the structural analysis, a state of plane strain was assumed. Two finite element analyses with the same discretization as the thermal model were performed. Conventional bilinear elements ( $P_S = 1$ ) and hierarchical biquadratic elements ( $P_S = 2$ ) were used for the analyses. Figure 19 shows comparative displacement distributions along the mirror surface. The hierarchical elements ( $P_S = 2$ ) provide a smooth displacement distribution whereas relatively high discontinuities of displacement gradients are produced by the conventional elements ( $P_S = 1$ ). Such discontinuities indicate the need for mesh refinement if conventional elements are to be used.

Thermal stress distributions along the middle plane of the mirror are shown in Figure 20. The conventional elements produce element stress discontinuities whereas a more realistic stress distribution is obtained from the hierarchical elements. The thermal stresses from the hierarchical analysis show small discontinuities indicating that solution convergence is not fully attained for  $P_S = 2$ , suggesting the need for including additional hierarchical terms. However, the principal advantage of using the hierarchical elements is clearly demonstrated by this example. Enhanced dis-



(a) IN-PLANE TEMPERATURE DISTRIBUTION (b) TRANSVERSE TEMPERATURE DISTRIBUTION

Figure 18. Typical temperature distributions at different mirror sections.

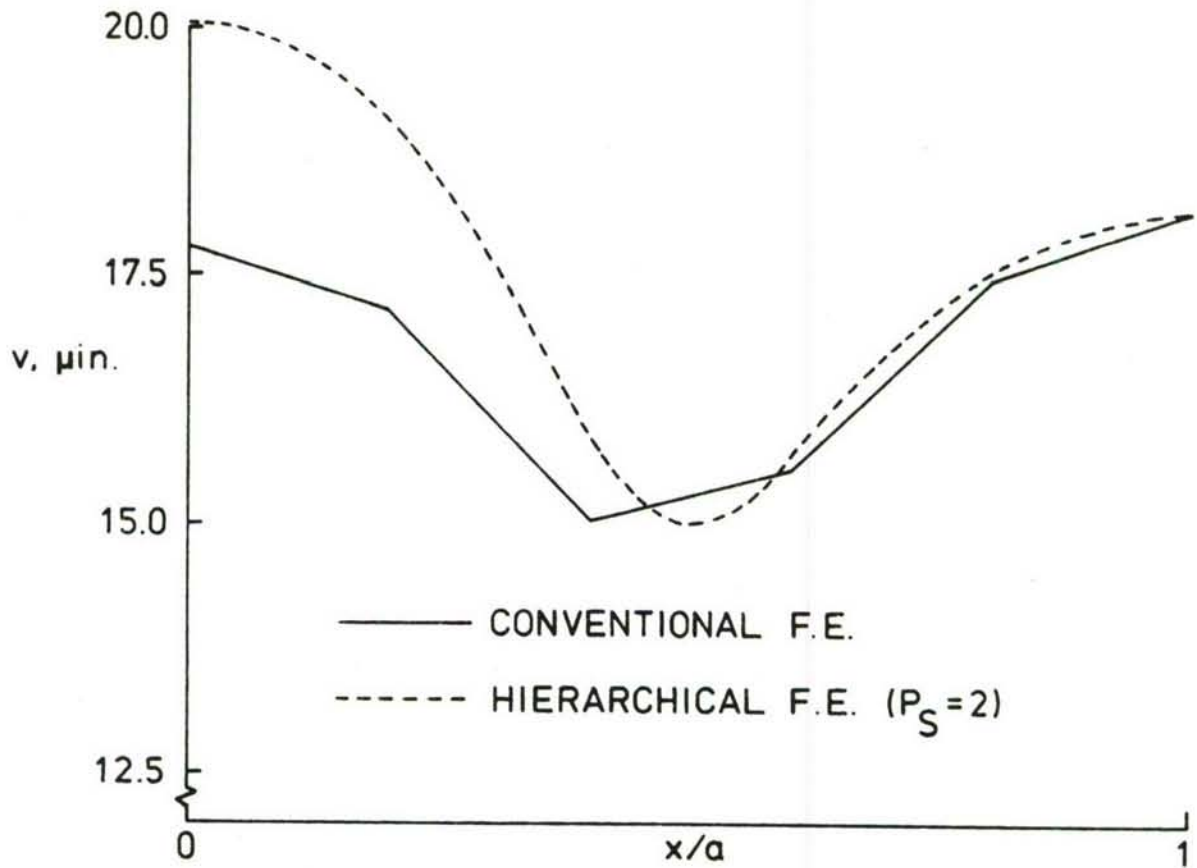
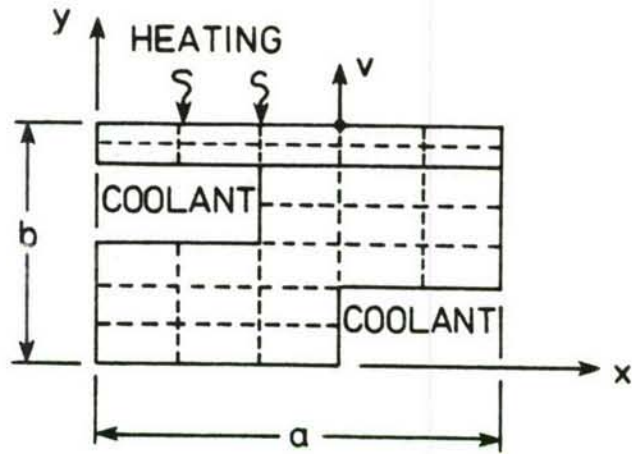


Figure 19. Comparative transverse displacement distributions along mirror surface.

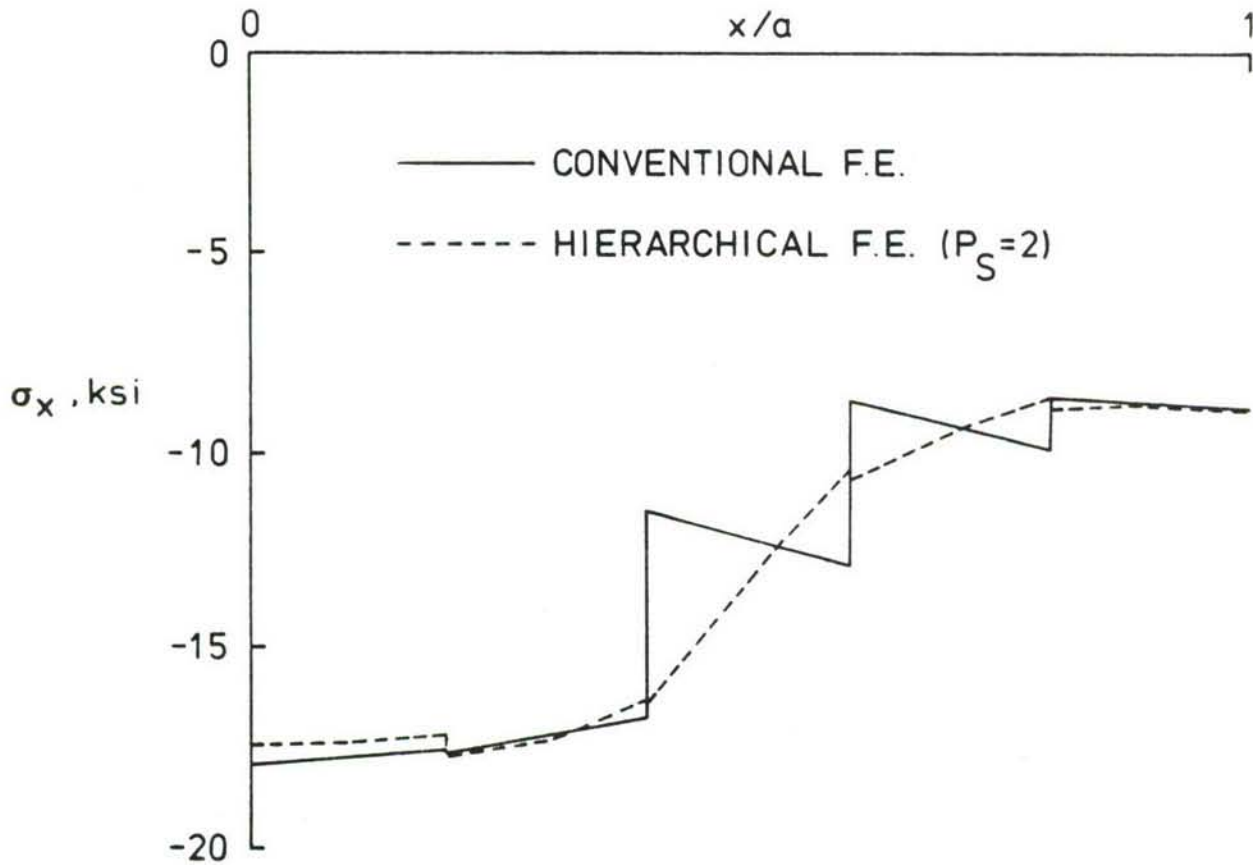
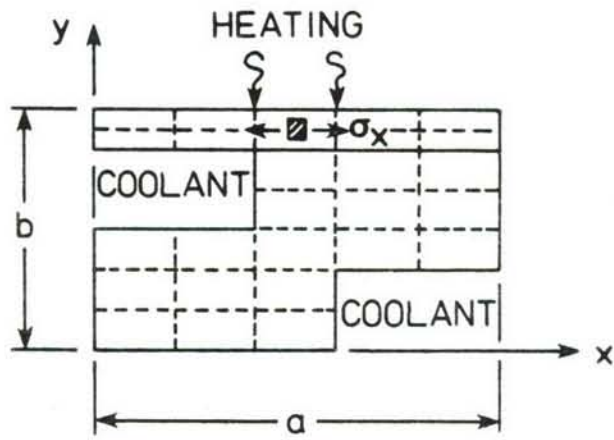


Figure 20. Comparative mirror in-plane stress distributions.

placement and thermal-stress solutions were obtained for a common geometric model.

SECTION VI  
CONCLUDING REMARKS

An integrated approach for enhanced thermal-structural analysis was presented. The approach focuses on applications where thermal and structural models often differ because of different analysis requirements. The objectives of the approach are to provide more efficient coupling between the thermal and structural analysis and to improve the accuracy of each analysis particularly the thermal-stress analysis. The integrated approach is based on using the same geometric model with a common nodal discretization for both analysis although the thermal and structural models can employ different elements to suit their different requirements.

Two approaches for integrating finite element thermal and structural analyses are presented. The first approach is based on applying the hierarchical concept of finite element approximation to both the thermal and structural analysis. In an hierarchical approach the accuracy of the finite element approximation is improved for the same mesh by increasing the order of interpolating functions and introducing additional unknowns via nodeless variables. The hierarchical approach to integrated thermal-structural analysis uses a common discretization for the thermal and structural analysis and seeks improvements in the accuracy of the thermal and structural analyses by independently refining the solutions using hierarchical interpolation functions for successive analyses. A key step in coupling the analyses is to use the converged temperature distribution to compute the finite element equivalent thermal forces. The second approach, called a nodeless parameter approach, uses a common discretization for both analyses and uses hierarchical interpolation functions to converge the thermal solution. The

structural analysis is based on using new temperature-dependent displacement interpolation functions that have element temperatures as parameters. Interpolation functions are presented for a rectangular element, and the generalization for a quadrilateral is briefly discussed. The use of the new interpolation functions can improve the accuracy of the structural analysis without adding extra unknowns.

Four two-dimensional examples are presented to illustrate the two approaches. Rectangular elements with bilinear interpolation functions are used for the initial analyses, and refinements of the analyses are made using the hierarchical approach or the nodeless parameter approach. Improvements in the accuracy of temperature and thermal-stresses were demonstrated in all examples.

The hierarchical approach offers the greatest potential for developing a general integrated thermal-structural analysis method. Maximum flexibility is permitted for independently improving the finite element approximation for each analysis while maintaining a common discretization and the analyses can be consistently coupled through the equivalent thermal forces. Additional study is needed to: (1) gain experience with higher order interpolation functions, (2) develop error estimation techniques to quantify convergence, and (3) study computer implementation techniques. The nodeless parameter approach offers the advantage of improving the accuracy of the structural analysis without adding unknowns. The approach, however, needs additional development before it can be implemented for general elements.

The integrated thermal-stress analysis approach based on hierarchical elements provides capability to improve accuracy and efficiency of thermal-stress analysis of complex structures. The examples presented in this

report validate some basic features of the approach for two-dimensional thermal stress problems, but additional research is needed to develop the approach to its full potential.

## REFERENCES

1. E. A. Thornton, P. Dechaumphai, and A. R. Wieting, Integrated Thermal-Structural Finite Element Analysis. Proceedings of the AIAA/ASME/ASCE/AHS 21st Structures, Structural Dynamics and Materials Conference, Seattle, Washington, AIAA Paper No. 80-0717, May 12-14, 1980.
2. E. A. Thornton, P. Dechaumphai, A. R. Wieting, and K. K. Tamma, Integrated Transient Thermal-Structural Finite Element Analysis. Proceedings of the AIAA/ASME/ASCE/AHS 22nd Structures, Structural Dynamics and Materials Conference, Atlanta, Georgia, AIAA Paper No. 81-0480, April 6-8, 1981.
3. E. A. Thornton, P. Dechaumphai, and A. R. Wieting, Integrated Finite Element Thermal-Structural Analysis with Radiation Heat Transfer, Proceedings of the AIAA/ASME/ASCE/AHS 23rd Structures, Structural Dynamics and Materials Conference, New Orleans, Louisiana, AIAA Paper No. 82-0703, May 10-12, 1982.
4. P. Dechaumphai, and E. A. Thornton, Nodeless Variable Finite Elements for Improved Thermal-Structural Analysis, Proceedings of the International Conference on Finite Element Methods (edited by H. Guangqian and Y. K. Cheung), Shanghai, China, August 2-6, 1982, Gordon and Breach Science Publishers, N. Y., pp. 139-144.
5. P. Dechaumphai, and E. A. Thornton, Improved Finite Element Methodology for Integrated Thermal Structural Analysis, NASA Contractor Report 3635, November 1982.
6. K. H. Huebner and E. A. Thornton, The Finite Element Method for Engineers, second edition, John Wiley and Sons, 1982.
7. O. C. Zienkiewicz and K. Morgan, Finite Elements and Approximation, John Wiley and Sons, 1983.
8. A. Peano, Hierarchies of Conforming Finite Elements for Plane Elasticity and Plate Bending, *Comput. Maths. with Appl.* Vol. 2, 1976, pp. 221-224.
9. M. P. Rossow and I. N. Katz, Hierarchical Finite Elements and Precomputed Arrays, *International Journal for Numerical Methods in Engineering*, Vol. 12, 1978, pp. 977-999.
10. O. C. Zienkiewicz, J. P. de S. R. Gago, and D. W. Kelly, The Hierarchical Concept in Finite Element Analysis, *Computers and Structures*, Vol. 16, pp. 53-65, 1983.
11. S. Timoshenko and J. N. Goodier, Theory of Elasticity, McGraw-Hill, 1951.

## LIST OF SYMBOLS

a	Surface absorptivity
$[\bar{B}]$	Nodeless parameter strain-displacement interpolation matrix
$[B_S]$	Strain-displacement interpolation matrix
$[B_T]$	Temperature gradient interpolation matrix
c	Specific heat
$[C]$	Finite element capacitance matrix
$[D]$	Elasticity matrix
E	Modulus of elasticity
$\{F_P\}$	Finite element nodal thermal force vector
$\{F_T\}$	Finite element nodeless parameter thermal force vector
$[k]$	Thermal conductivity matrix
$[K_C]$	Finite element conduction matrix
$[K_r]$	Finite element radiation matrix
$[K_S]$	Finite element stiffness matrix
$[N]$	Finite element interpolation function matrix
$[\bar{N}]$	Finite element nodeless parameter interpolation function matrix
$[N_S]$	Finite element displacement interpolation function matrix
$[N_T]$	Finite element temperature interpolation function matrix
$P_T$	Order of interpolating polynomial for thermal analysis
$P_S$	Order of interpolating polynomial for structural analysis
q	Surface heating rate

$q_r$	Surface incident radiation heating rate
$\{Q_q\}$	Finite element surface heating load vector
$\{Q_r\}$	Finite element radiation heating load vector
$t$	Time
$T$	Temperature
$T_{ref}$	Reference temperature for zero stress
$u, v, w$	Displacement components
$V$	Volume
$x, y, z$	Cartesian coordinates
$\{\alpha\}$	Vector of thermal expansion coefficients
$\{\delta\}$	Vector of finite element nodal displacements
$\rho$	Mass density
$\sigma$	Stefan-Boltzmann constant
$\epsilon$	Surface emissivity
$\{\epsilon\}$	Vector of finite element total strains
$\{\epsilon_0\}$	Vector of finite element thermal strains
$\{\sigma\}$	Vector of finite element stresses
$\nu$	Poisson's ratio
$\Pi$	Internal strain energy
$\xi, \eta, \zeta$	Finite element natural coordinates